International Conference 50 Years of Cold Fusion
Yerevan, Nov. 19-24, 2024

Structure and fission properties of heavy and superheavy nuclei

Shan-Gui Zhou (周善贵)

Institute of Theoretical Physics, Chinese Academy of Sciences, Beijing
University of Chinese Academy of Sciences, Beijing

Supported by: NSFC & MOST;
HPC Cluster of KLFTP/ITP-CAS
ScGrid of CNIC-CAS

CAS & ITP

- CAS: Chinese Academy of Sciences
  - >100 institutes & 3 universities in China; >40 in Beijing
  - ~45,000 graduate students for Master's or PhD degrees

- ITP: Institute of Theoretical Physics, Beijing
  - Founded in 1978 & the smallest one in CAS
  - 52 (assistant, associate & full) professors + ~50 postdocs + ~150 students
  - Atomic physics; Nuclear physics; Particle physics; String theory; Cosmology; Condensed matter physics; Biophysics; Statistical physics; Quantum physics & quantum information; ...

Contents

Nuclear shapes

$$R(\theta,\varphi) = R_0\left[1 + \beta_{00} + \sum_{\lambda=1}^{\infty}\sum_{\mu=-\lambda}^{\lambda}\beta^*_{\lambda\mu}Y_{\lambda\mu}(\theta,\varphi)\right]$$

2^λ-pole deformation (2^λ-极形变)

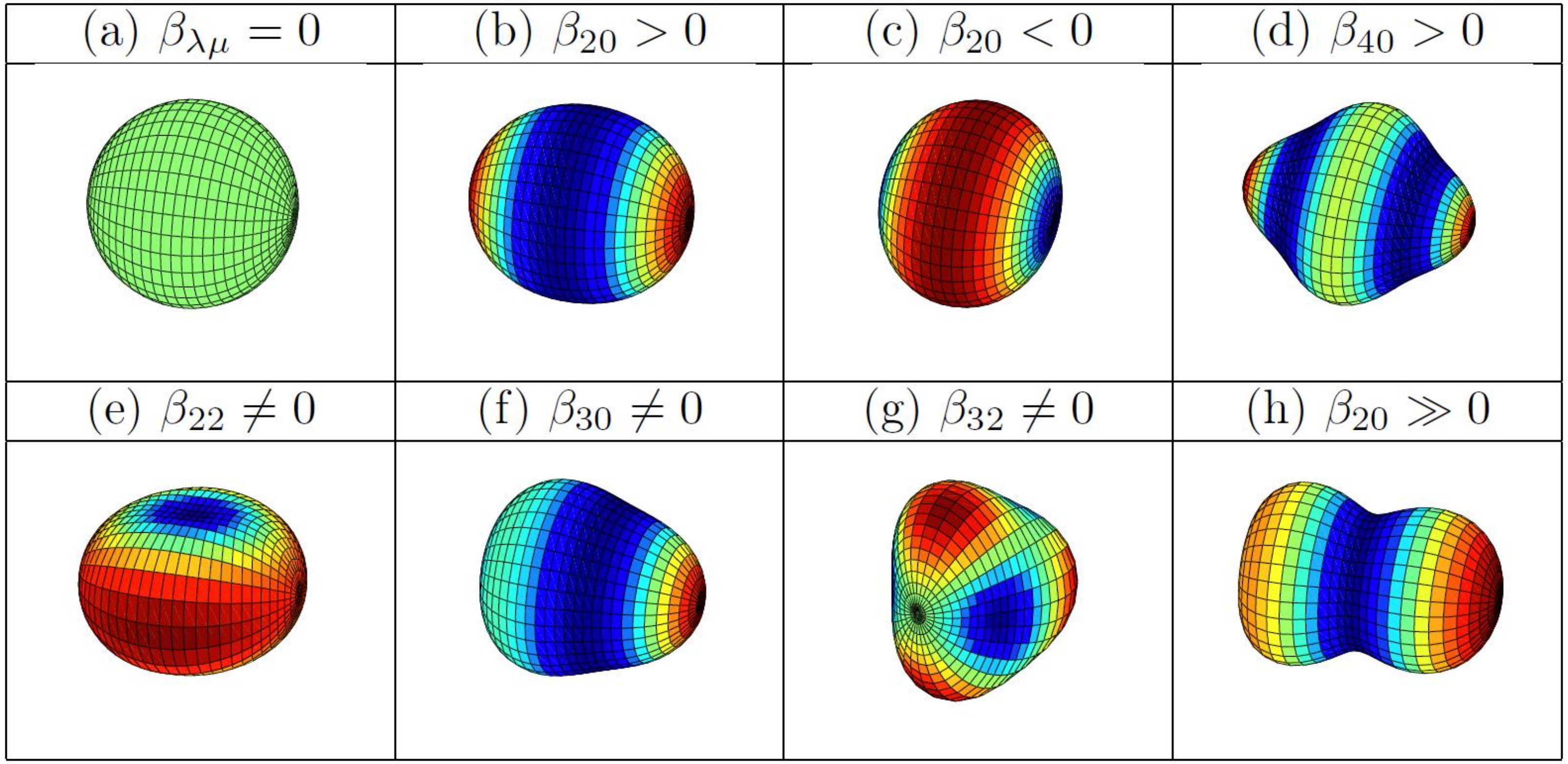

Courtesy of Bing-Nan Lu (吕炳楠)

Nonaxial quadrupole shape (β_{22} or γ)

J. Phys. G: Nucl. Part. Phys. **37** (2010) 064025

Meng_Zhang 2010_JPG37-064025

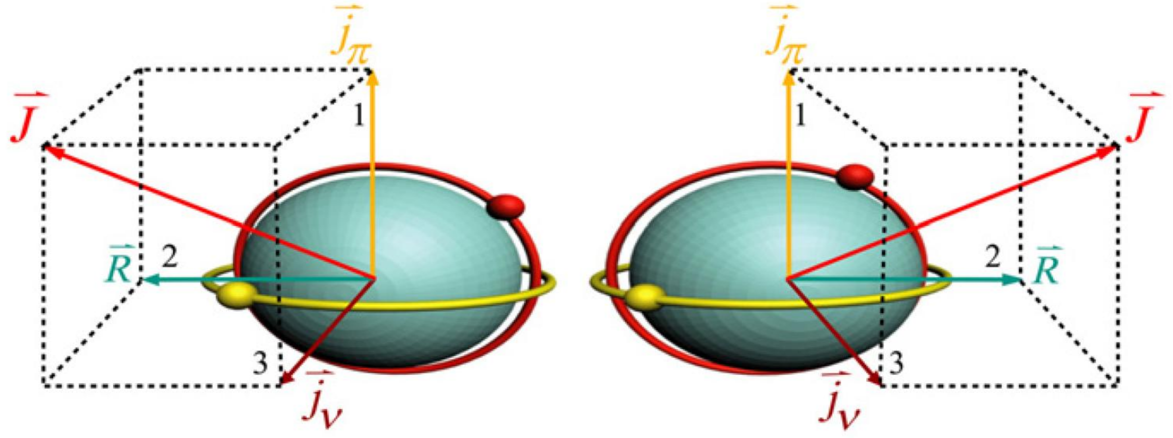

Figure 1. Left- and right-handed chiral systems for a triaxial odd–odd nucleus.

A static triaxial shape in atomic nuclei manifests itself by

the wobbling motion & chiral doublet bands

Bohr & Mottelson 1975
Odegard+2001_PRL86-5866
…

Frauendorf_Meng1997_NPA617-131
Starosta+2001_PRL86-971
…

Octupole shape (β_{30})

Gaffney_Butler_Scheck+2013_Nature497-199

ARTICLE

doi:10.1038/nature12073

Studies of pear-shaped nuclei using accelerated radioactive beams

L. P. Gaffney[1], P. A. Butler[1], M. Scheck[1,2], A. B. Hayes[3], F. Wenander[4], M
N. Bree[7], J. Cederkäll[8], T. Chupp[9], D. Cline[3], T. E. Cocolios[4], T. Davinson
M. Huyse[7], D. G. Jenkins[13], D. T. Joss[1], N. Kesteloot[7,11], J. Konki[12], M. Kowa
P. Napiorkowski[14], J. Pakarinen[4,12], M. Pfeiffer[5], D. Radeck[5], P. Reiter[5], K
S. Sambi[7], M. Seidlitz[5], B. Siebeck[5], T. Stora[4], P. Thoele[5], P. Van Duppen[7], N
K. Wimmer[18], K. Wrzosek-Lipska[7,14], C. Y. Wu[15] & M. Zielinska[14,19]

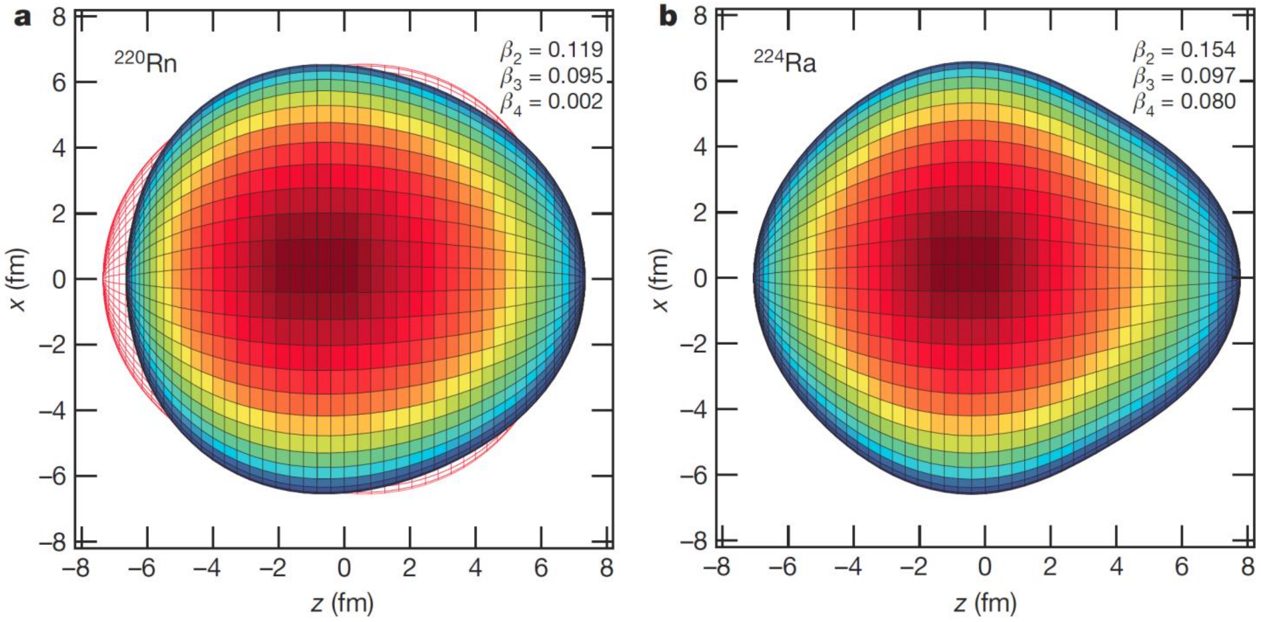

Nuclear fission

- Fission barrier is crucial for the description of fission
- Various shapes may appear during fission

$$R(\theta,\varphi) = R_0\left[1+\beta_{00}+\sum_{\lambda=1}^{\infty}\sum_{\mu=-\lambda}^{\lambda}\beta^{*}_{\lambda\mu}Y_{\lambda\mu}(\theta,\varphi)\right]$$

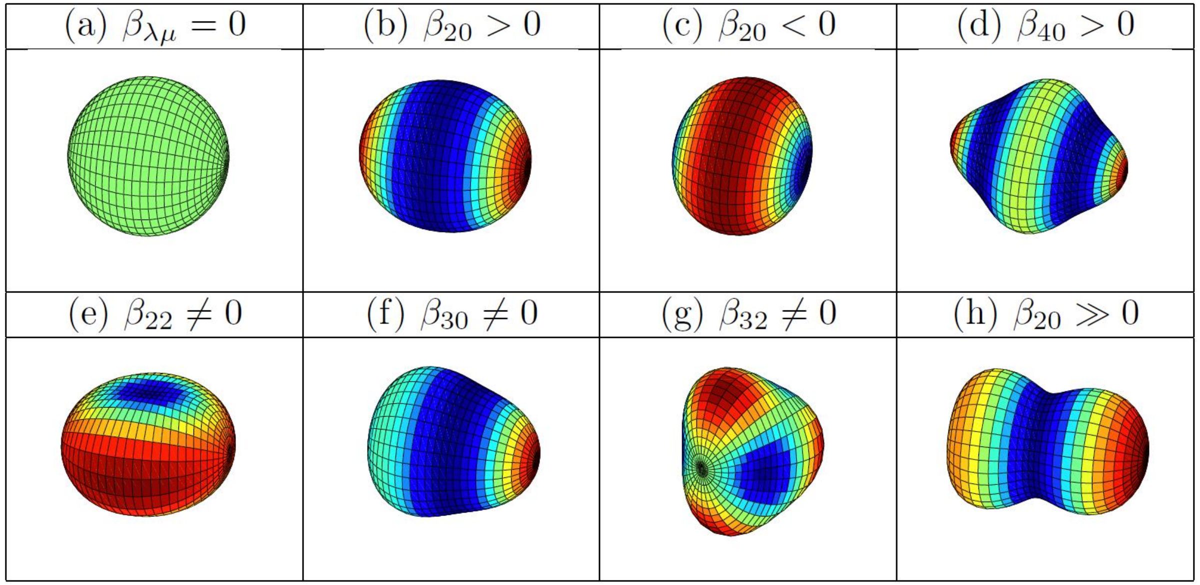

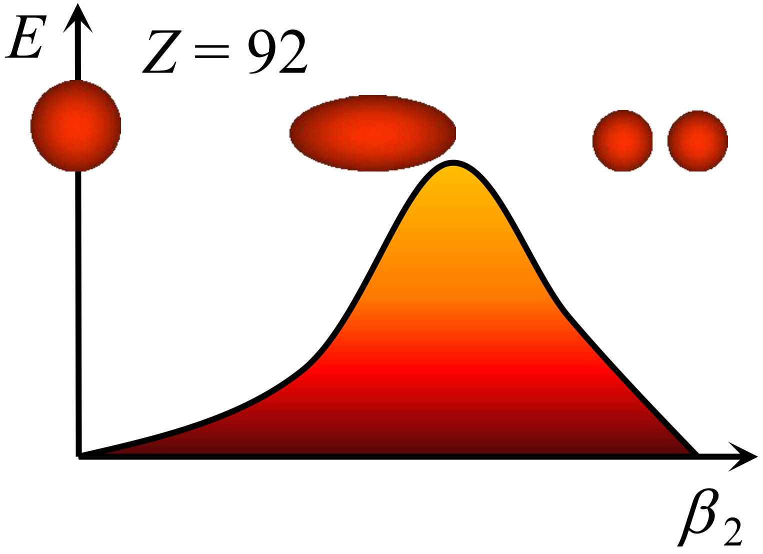

$\{\beta_2, \beta_4, \cdots\}$

2^{λ}-pole deformation (2^{λ}-极形变)

Nonaxial (β_{22} or γ) & octupole (β_{30}) shapes in PES

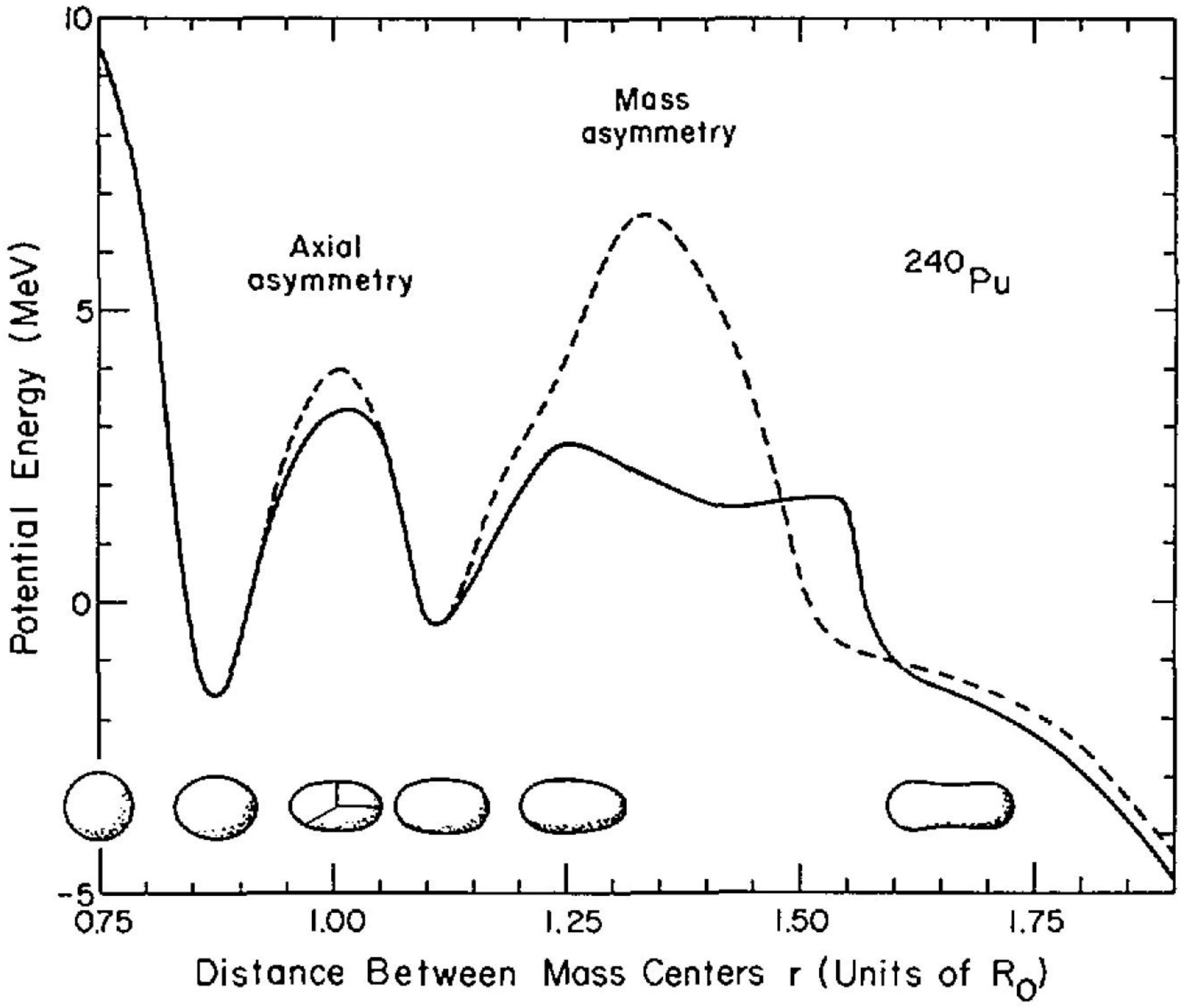

Möller_Nix 1973
IAEA-SM-174/202

Nonaxial (β_{22} or γ) & octupole (β_{30}) shapes in PES

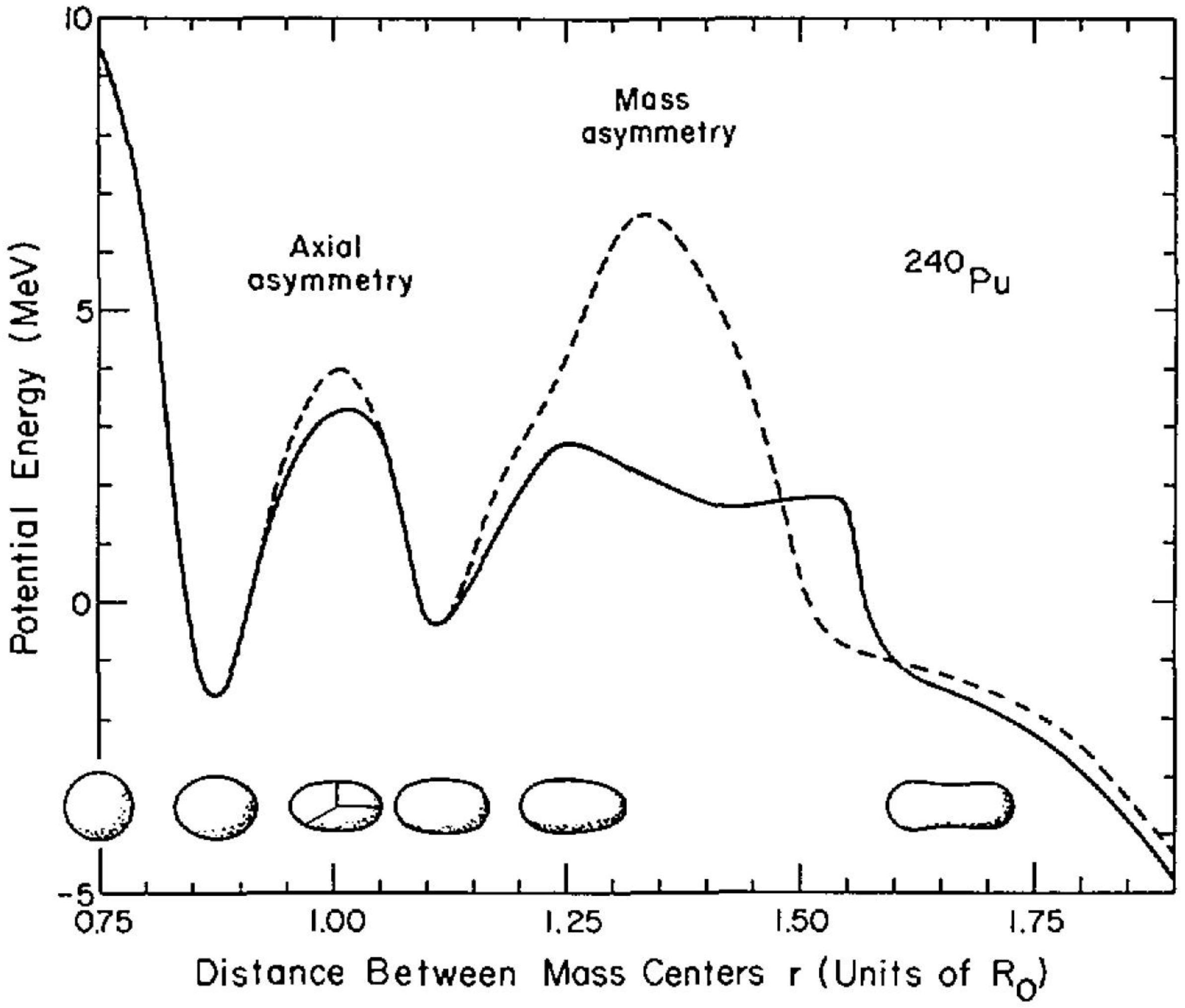

Möller_Nix 1973
IAEA-SM-174/202

Axial asymmetry plays important roles around the first barrier

Reflection asymmetry plays important roles around the second barrier

Nonaxial (β_{22} or γ) & octupole (β_{30}) shapes in PES

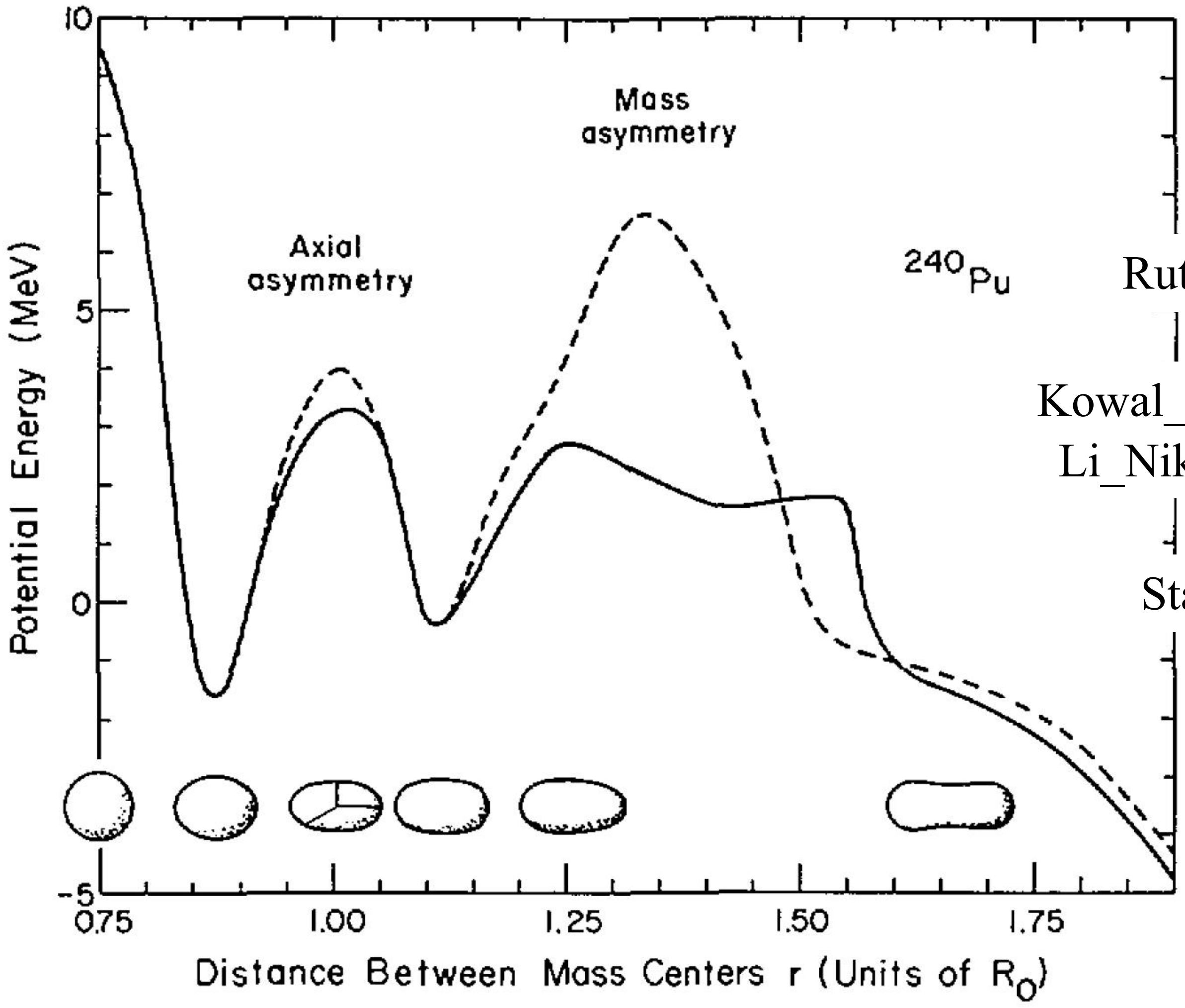

Möller_Nix 1973
IAEA-SM-174/202

Pashkevich1969_NPA133-400
Rutz_Maruhn_Reihard_Greiner1995_NPA590-680
Robledo_Warda2008_IJMPE17-204
Kowal_Jachikowicz_Sobiczewski2010_PRC82-014303
Li_Niksic_Vretenar_Ring_Meng2010_PRC81-064321
Abusara_Afanasjev_Ring2010_PRC82-044303
Staszczak_Baran_Nazarewicz2011_IJMPE20-552
Royer_Jaffre_Moreau2012_PRC86-044326
…

Axial asymmetry plays important roles around the first barrier
Reflection asymmetry plays important roles around the second barrier

Covariant Density Functional Theory (CDFT)

$$\begin{aligned}\mathcal{L} = & \bar{\psi}_i (i\partial\!\!\!/ - M)\psi_i + \frac{1}{2}\partial_\mu\sigma\partial^\mu\sigma - U(\sigma) - g_\sigma\bar{\psi}_i\sigma\psi_i \\ & - \frac{1}{4}\Omega_{\mu\nu}\Omega^{\mu\nu} + \frac{1}{2}m_\omega^2\omega_\mu\omega^\mu - g_\omega\bar{\psi}_i\omega\!\!\!/\psi_i \\ & - \frac{1}{4}\vec{R}_{\mu\nu}\vec{R}^{\mu\nu} + \frac{1}{2}m_\rho^2\vec{\rho}_\mu\vec{\rho}^\mu - g_\rho\bar{\psi}_i\vec{\rho\!\!\!/}\vec{\tau}\psi_i \\ & - \frac{1}{4}F_{\mu\nu}F^{\mu\nu} - e\bar{\psi}_i\frac{1-\tau_3}{2}A\!\!\!/\psi_i,\end{aligned}$$

$$(\boldsymbol{\alpha}\cdot\mathbf{p} + \beta(M + S(\mathbf{r})) + V(\mathbf{r}))\psi_i = \epsilon_i\psi_i$$

$$\left(-\nabla^2 + m_\sigma^2\right)\sigma = -g_\sigma\rho_S - g_2\sigma^2 - g_3\sigma^3$$

$$\left(-\nabla^2 + m_\omega^2\right)\omega = g_\omega\rho_V - c_3\omega^3$$

$$\left(-\nabla^2 + m_\rho^2\right)\rho = g_\rho\rho_3$$

$$-\nabla^2 A = e\rho_C$$

Serot_Walecka1986_ANP16-1

Reinhard1989_RPP52-439

Ring1996_PPNP37-193

Vretenar_Afanasjev_Lalazissis_Ring2005_PR409-101

Meng_Toki_SGZ_Zhang_Long_Geng2006_PPNP57-470

Liang_Meng_SGZ2015_PR570-1

Meng_SGZ2015_JPG42-093101

Meng (ed.), Relativistic Density Functional for Nuclear structure (World Scientific, 2016)

MDC-CDFTs (β_{20}, β_{22}, β_{30}, β_{32}, β_{40}, …)

- Axially deformed harmonic oscillator (ADHO) basis

Ring_Gambhir_Lalazissis1997_CPC105-77

$$\left[-\frac{\hbar^2}{2M}\nabla^2 + V_B(z,\rho)\right]\Phi_\alpha(\boldsymbol{r}\sigma) = E_\alpha \Phi_\alpha(\boldsymbol{r}\sigma)$$

$$V_B(z,\rho) = \frac{1}{2}M(\omega_\rho^2\rho^2 + \omega_z^2 z^2)$$

$$\Phi_\alpha(\boldsymbol{r}\sigma) = C_\alpha \phi_{n_z}(z) R_{n_\rho}^{m_l}(\rho)\frac{1}{\sqrt{2\pi}}e^{im_l\varphi}\chi_{s_z}(\sigma)$$

- Fourier expansion for densities & potentials

$$f(\rho,\varphi,z) = f_0(\rho,z)\frac{1}{\sqrt{2\pi}} + \sum_{n=1}^{\infty} f_n(\rho,z)\frac{1}{\sqrt{\pi}}\cos(2n\varphi)$$

$$f = V \text{ or } \rho$$

- A modified linear constraint method

$$E' = E_{\mathrm{RMF}} + \sum_{\lambda\mu}\frac{1}{2}C_{\lambda\mu}Q_{\lambda\mu}$$

$$C_{\lambda\mu}^{(n+1)} = C_{\lambda\mu}^{(n)} + k_{\lambda\mu}\left(\beta_{\lambda\mu}^{(n)} - \beta_{\lambda\mu}\right)$$

Lu_Zhao_Zhao_SGZ 2014_PRC89-014323   Zhao_Lu_Zhao_SGZ 2017_PRC95-014320

Applications of MDC-CDFTs

- Potential energy surface, ground state & fission properties
  - (β_{20}, β_{22}, β_{30}): 1-, 2- & 3-dim PES of ^{240}Pu & B_f's of actinides
  - (β_{20}, β_{22}): Shape polarization effect of Λ
  - (β_{20}): Superdeformed shapes in Λ hypernuclei
  - (β_{20}): Third barriers in light actinides
  - (β_{20}, β_{30}): Octupole correlations & shape transitions
  - (β_{20}, β_{22}, β_{30}): Octupole correlations in MχD
  - (β_{20}, β_{32}): Nuclear Tetrahedral shapes
  - (β_{20}, β_{22}, β_{30}): 1-, 2-, & 3-dim PES of ^{270}Hs & B_f's of even-even superheavies
  - ($\beta_{\lambda\mu}$, *R*): Clustering, bubble & toroidal structure; GMR
- Fission dynamics based on PES from MDC-CDFTs
  - Spontaneous fission
  - Induced fission
- Angular momentum & parity projected MDC-CDFTs
  - Clustering & exotic shapes

MultiDimensionally-Constrained Covariant Density Functional Theories

Collaborators

Xiang-Quan Deng (邓祥泉)	Univ. CAS
Emiko Hiyama	Kyushu Univ. & RIKEN
Shivani Jain	ITP/CAS
Zhi-Pan Li (李志攀)	Southwest Univ.
Bing-Nan Lu (吕炳楠)	Graduate School, China AEP
Xiao Lu (陆晓)	ITP/CAS
Xu Meng (孟旭)	Yanshan Univ.
Tamara Niksic	Univ. Zagreb
Yu-Ting Rong (荣宇婷)	Guangxi Normal Univ.
Hiroyuki Sagawa	RIKEN & Aizu Univ.
Xiang-Xiang Sun (孙向向)	Forschungszentrum Jülich
Dario Vretenar	Univ. Zagreb
Kun Wang (王琨)	
Xiao-Qian Wang (王晓倩)	ITP/CAS
Jiang Xiang (向剑)	Qiannan Normal Univ. Nationalities
En-Guang Zhao (赵恩广)	ITP/CAS
Jie Zhao (赵杰)	Pengcheng Lab

Applications of MDC-CDFTs

- Potential energy surface, ground state & fission properties
  - (β_{20}, β_{22}, β_{30}): 1-, 2- & 3-dim PES of ^{240}Pu & B_f's of actinides
  - (β_{20}, β_{22}): Shape polarization effect of Λ
  - (β_{20}): Superdeformed shapes in Λ hypernuclei
  - (β_{20}): Third barriers in light actinides
  - (β_{20}, β_{30}): Octupole correlations & shape transitions
  - (β_{20}, β_{22}, β_{30}): Octupole correlations in MχD
  - (β_{20}, β_{32}): Nuclear Tetrahedral shapes
  - (β_{20}, β_{22}, β_{30}): 1-, 2-, & 3-dim PES of ^{270}Hs & B_f's of even-even superheavies
  - ($\beta_{\lambda\mu}$, *R*): Clustering, bubble & toroidal structure; GMR
- Fission dynamics based on PES from MDC-CDFTs
  - Spontaneous fission
  - Induced fission
- Angular momentum & parity projected MDC-CDFTs
  - Clustering & exotic shapes

MultiDimensionally-Constrained Covariant Density Functional Theories

^{240}Pu: 3-dim. PES (β_{20}, β_{22}, β_{30})

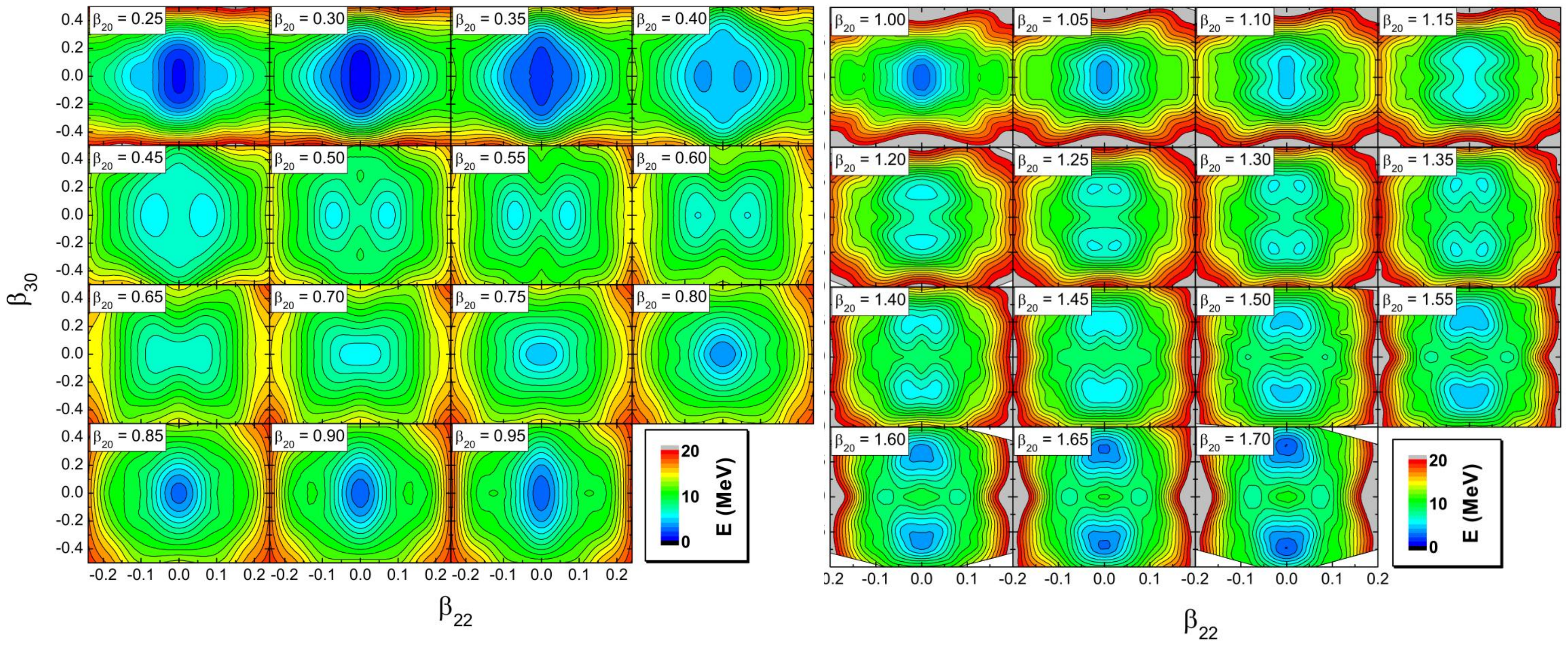

β_{20}: 0.25 to 1.70 w/ a step of 0.05
β_{22}: 0.00 to 0.25 w/ a step of 0.01
β_{30}: 0.00 to 0.50 w/ a step of 0.05

8580 points

Lu_Zhao_SGZ 2014_PRC89-014323

^{240}Pu: 3-dim. PES (β_{20}, β_{22}, β_{30})

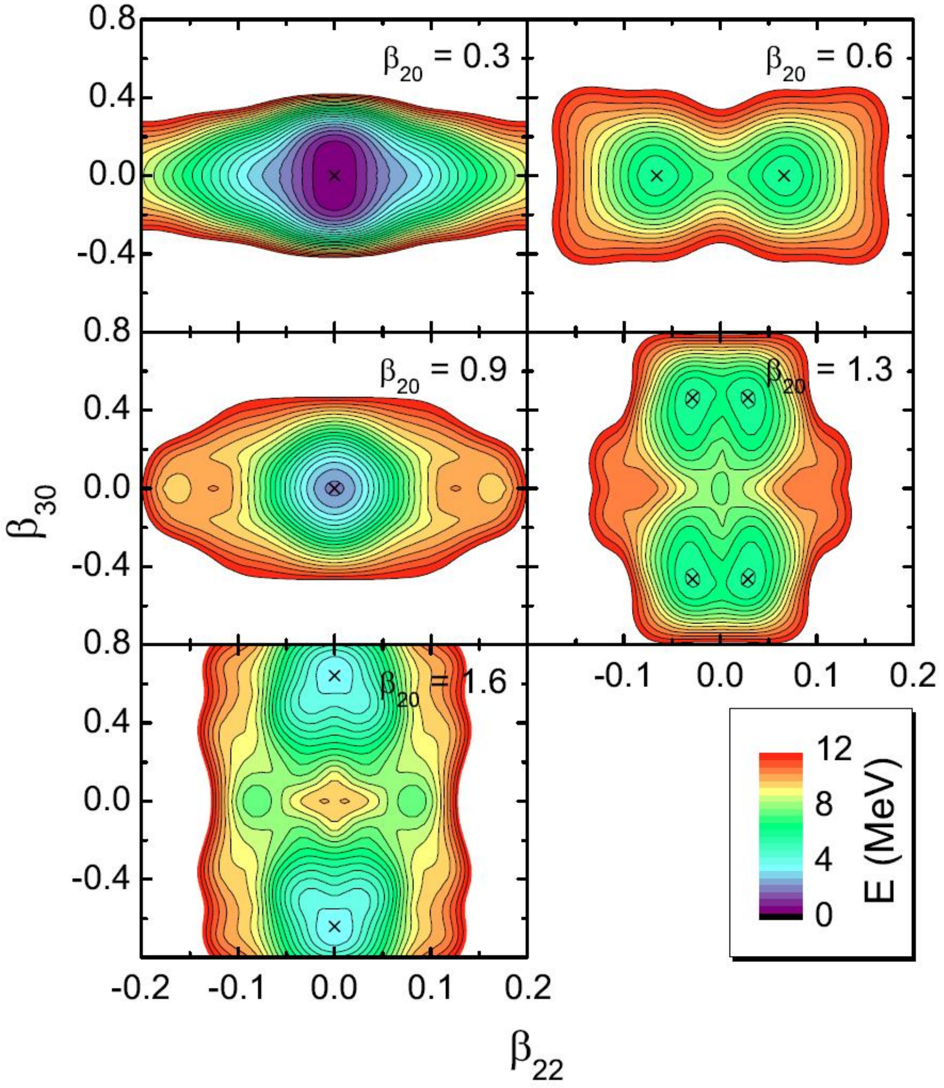

- AS & RS for g.s. & isomer, the latter is stiffer
- Triaxial & octupole shape around the outer barrier
- Triaxial deformation crucial around barriers

Lu_Zhao_SGZ 2012_PRC85-011301R

Lu_Zhao_SGZ 2014_PRC89-014323

^{240}Pu: 2-dim. PES (β_{20}, β_{30})

Without triaxility

With triaxility

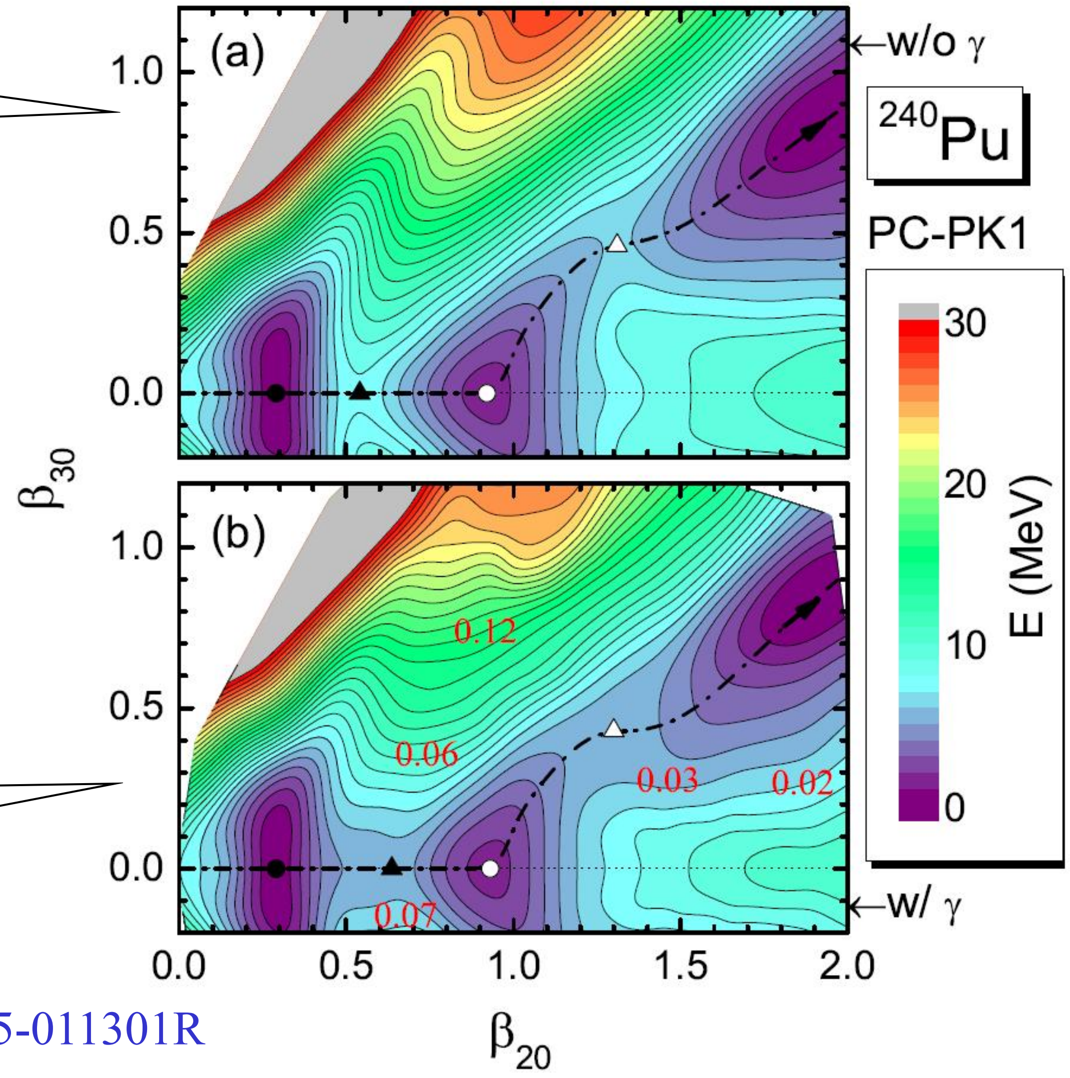

Lu_Zhao_SGZ 2012_PRC85-011301R

^{240}Pu: 1-dim. potential energy curve (β_{20})

- Triaxiality lowers inner barrier height by more than 2 MeV
- Octupole deformation lowers outer barrier dramatically
- Triaxiality lowers outer barrier height by about 1 MeV

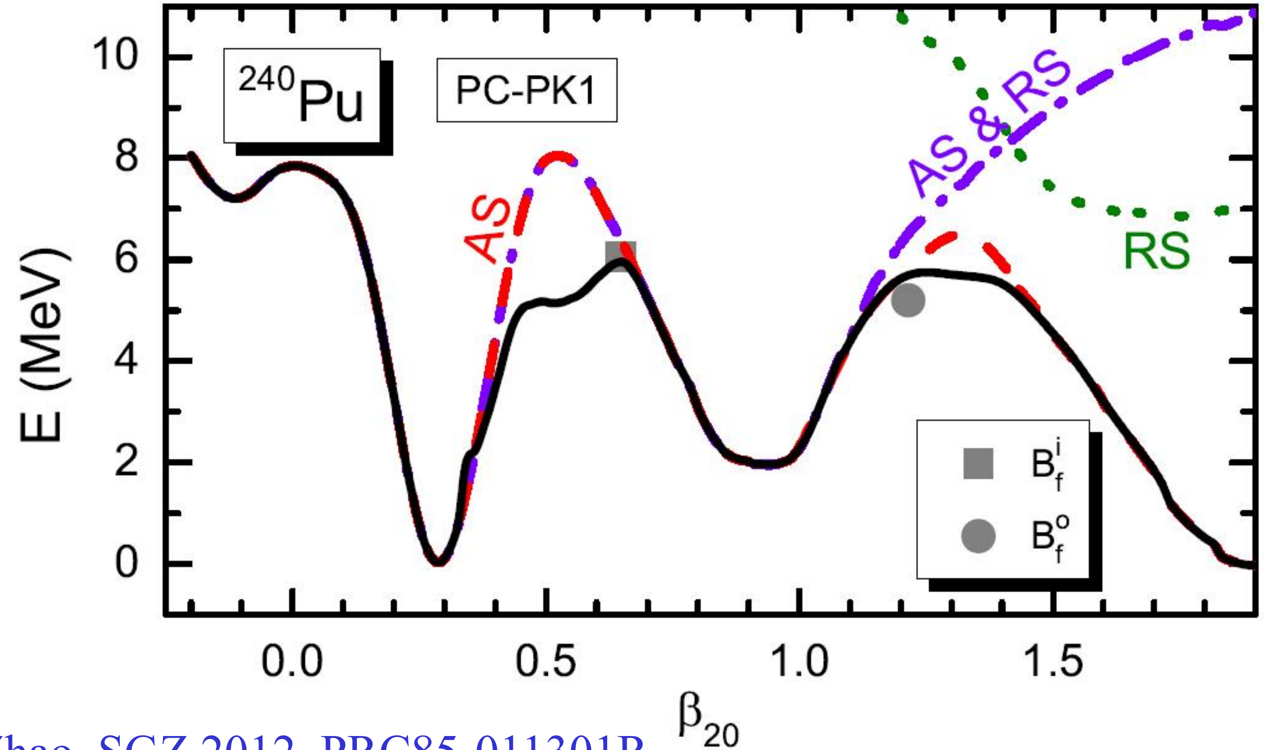

Lu_Zhao_SGZ 2012_PRC85-011301R

AS: Axially Sym.
RS: Reflection Sym.

B_f of actinide nuclei

Lu_Zhao_Zhao_SGZ 2014_PRC89-014323

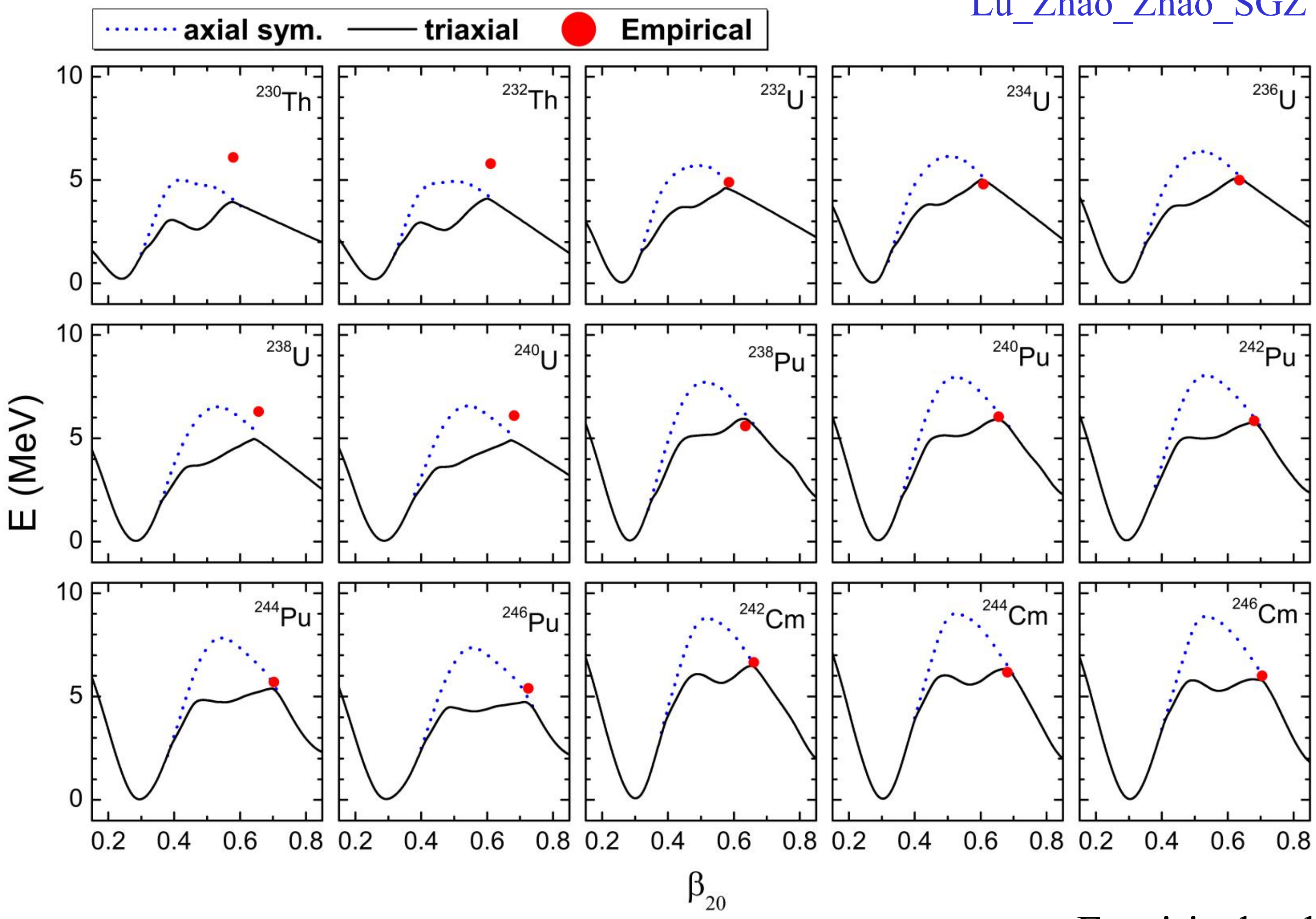

Around inner barriers

Empirical values: Capote…2009
NDC110-3107 (RIPL-3)

B_f of actinide nuclei

Lu_Zhao_Zhao_SGZ 2014_PRC89-014323

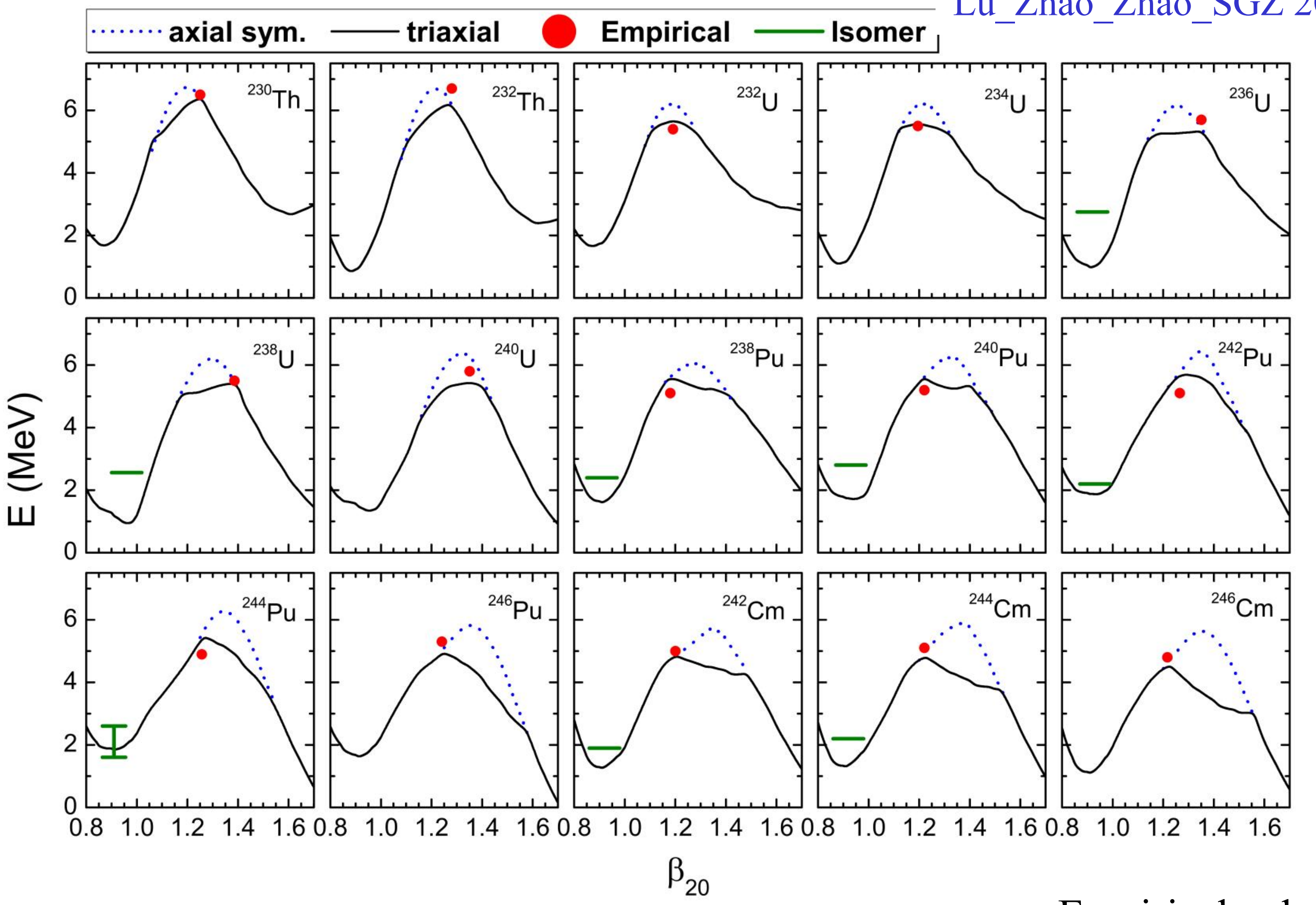

Around outer barriers

Empirical values: Capote…2009
NDC110-3107 (RIPL-3)

B_f of actinide nuclei

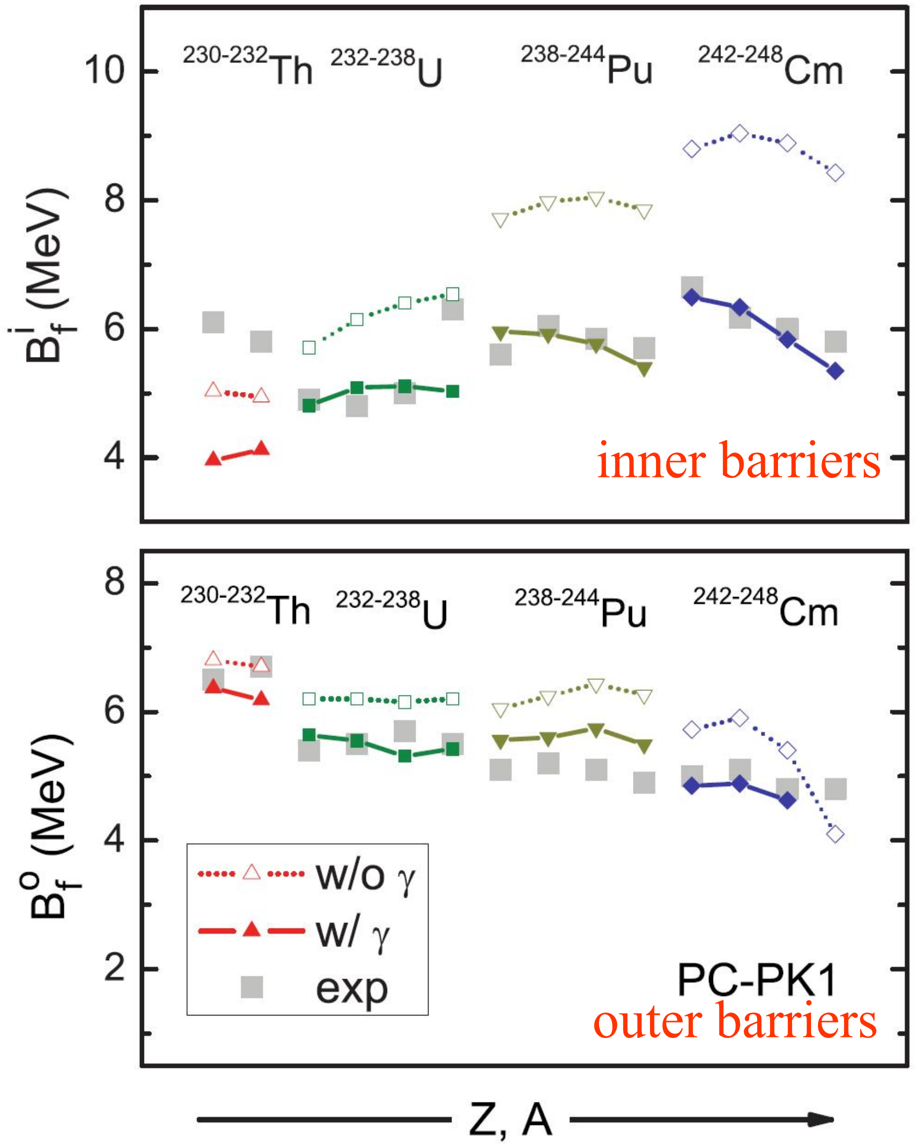

Lu_Zhao_SGZ 2012_PRC85-011301R

- Influence of triaxiality
  - Inner fission barriers lowered by 1~2 MeV
  - Outer fission barriers lowered by 0.5~1 MeV
- Problems
  - $^{230-232}$Th: out barriers primary
  - ^{238}U: ?
  - ^{248}Cm: two fission paths

Empirical values: Capote…2009
NDC110-3107 (RIPL-3)

B_f of actinide nuclei

Lu_Zhao_Zhao_SGZ 2014_PRC89-014323

Nucleus	Z	N	A	First barrier			Second barrier		
				AS	TA	Emp	AS	TA	Emp
^{230}Th	90	140	230	5.03	3.96	6.10	6.80	6.37	6.50
^{232}Th	90	142	232	4.94	4.12	5.80	6.70	6.18	6.70
^{232}U	92	140	232	5.71	4.81	4.90	6.20	5.64	5.40
^{234}U	92	142	234	6.15	5.09	4.80	6.20	5.55	5.50
^{236}U	92	144	236	6.40	5.11	5.00	6.15	5.31	5.70
^{238}U	92	146	238	6.54	5.03	6.30	6.20	5.42	5.50
^{240}U	92	148	240	6.58	4.96	6.10	6.38	5.43	5.80
^{238}Pu	94	144	238	7.72	5.96	5.60	6.05	5.56	5.10
^{240}Pu	94	146	240	7.98	5.92	6.05	6.24	5.60	5.20
^{242}Pu	94	148	242	8.05	5.77	5.85	6.43	5.74	5.10
^{244}Pu	94	150	244	7.85	5.40	5.70	6.26	5.49	4.90
^{246}Pu	94	152	246	7.37	4.76	5.40	5.84	4.96	5.30
^{242}Cm	96	146	242	8.80	6.49	6.65	5.72	4.85	5.00
^{244}Cm	96	148	244	9.04	6.34	6.18	5.90	4.88	5.10
^{246}Cm	96	150	246	8.89	5.84	6.00	5.40	4.62	4.80
^{248}Cm	96	152	248	8.43	5.35	5.80	4.10	—	4.80
^{250}Cm	96	154	250	7.77	4.79	5.40	2.60	—	4.40
^{250}Cf	98	152	250	8.87	5.70	5.60	2.40	—	3.80
^{252}Cf	98	154	252	8.41	5.26	5.30	1.20	—	3.50

Empirical values: Capote…2009
NDC110-3107 (RIPL-3)

B_f of actinide nuclei

PC-PK1

Lu_Zhao_Zhao_SGZ 2014_PRC89-014323

Nucleus	Z	N	A	First barrier			Second barrier		
				AS	TA	Emp	AS	TA	Emp
^{230}Th	90	140	230	5.03	3.96	6.10	6.80	6.37	6.50
^{232}Th	90	142	232	4.94	4.12	5.80	6.70	6.18	6.70
^{232}U	92	140	232	5.71	4.81	4.90	6.20	5.64	5.40
^{234}U	92	142	234	6.15	5.09	4.80	6.20	5.55	5.50
^{236}U	92	144	236	6.40	5.11	5.00	6.15	5.31	5.70
^{238}U	92	146	238	6.54	5.03	6.30	6.20	5.42	5.50
^{240}U	92	148	240	6.58	4.96	6.10	6.38	5.43	5.80
^{238}Pu	94	144	238	7.72	5.96	5.60	6.05	5.56	5.10
^{240}U	92	148	240	6.58	4.96	6.10	6.38	5.43	5.80
^{244}Pu	94	150	244	7.85	5.40	5.70	6.26	5.49	4.90
^{246}Pu	94	152	246	7.37	4.76	5.40	5.84	4.96	5.30
^{242}Cm	96	146	242	8.80	6.49	6.65	5.72	4.85	5.00
^{244}Cm	96	148	244	9.04	6.34	6.18	5.90	4.88	5.10
^{246}Cm	96	150	246	8.89	5.84	6.00	5.40	4.62	4.80
^{248}Cm	96	152	248	8.43	5.35	5.80	4.10	—	4.80
^{250}Cm	96	154	250	7.77	4.79	5.40	2.60	—	4.40
^{250}Cf	98	152	250	8.87	5.70	5.60	2.40	—	3.80
^{252}Cf	98	154	252	8.41	5.26	5.30	1.20	—	3.50

Nishio (FUSION17):

$B_f = 5.5$ MeV for ^{240}U

Empirical values: Capote…2009
NDC110-3107 (RIPL-3)

^{270}Hs: A doubly magic deformed SHN

Möller_Nilsson_Nix1974_NPA229-292
Čwiok_Pashkevich_Dudek_Nazarewicz1983_NPA410-254
Möller_Leander_Nix1986_ZPA323-41
Sobiczewski_Patyk_Čwiok1987_PLB186-6
Patyk_Skalski_Sobiczewski_Cwiok1989_NPA502-591c
Patyk_Sobiczewski1991_NPA533-132

^{270}Hs: A doubly magic deformed SHN

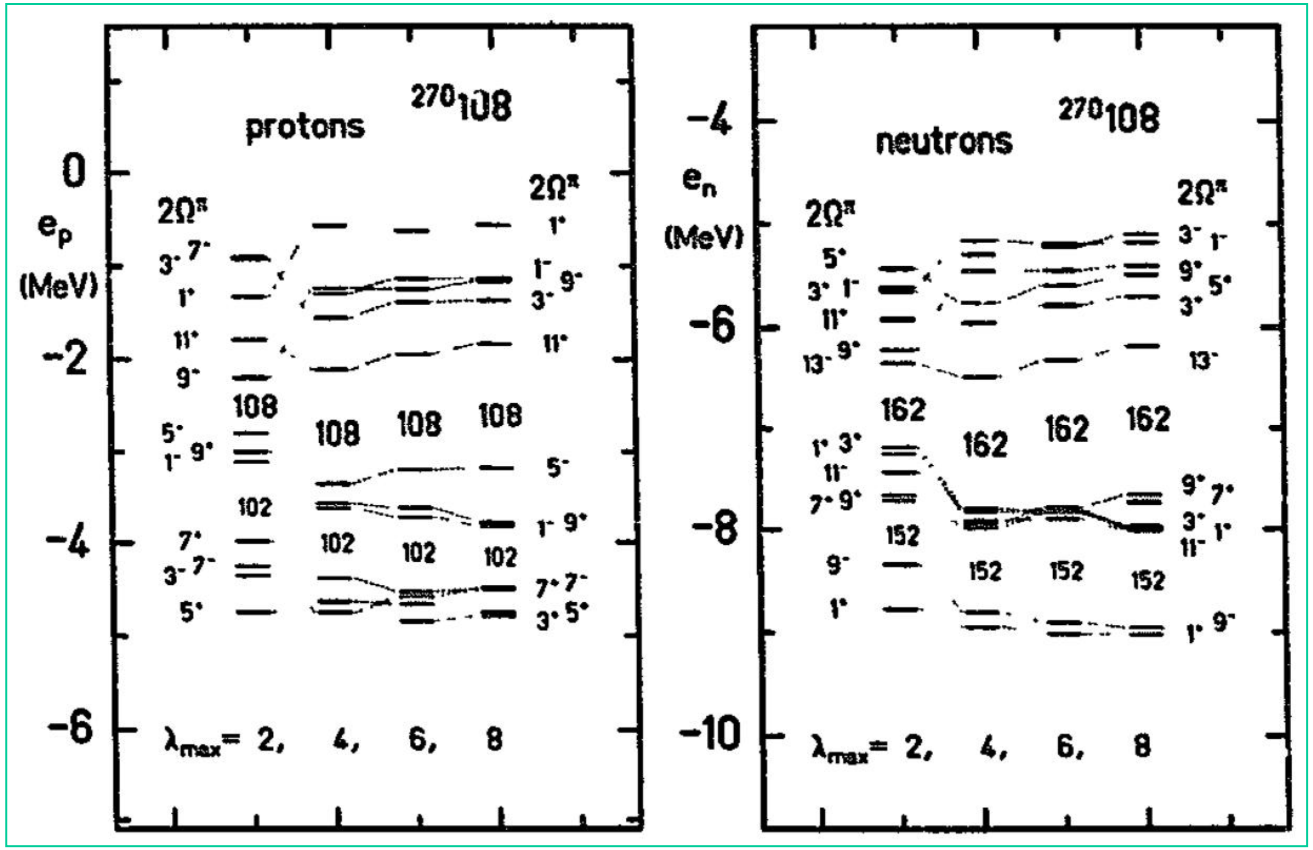

Möller_Nilsson_Nix1974_NPA229-292
Čwiok_Pashkevich_Dudek_Nazarewicz1983_NPA410-254
Möller_Leander_Nix1986_ZPA323-41
Sobiczewski_Patyk_Čwiok1987_PLB186-6
Patyk_Skalski_Sobiczewski_Cwiok1989_NPA502-591c
Patyk_Sobiczewski1991_NPA533-132

Patyk_Sobiczewski1991_NPA533-132

^{270}Hs: ground state properties

	E_B (MeV)	β_2	R_c (fm)	R_m (fm)
MDC-RMF (PC-PK1)	1967.40	0.261	6.167	6.23
AME2016 [140–142]	1969.65			
MMM [40]	1969.20	0.229		
RMF (TMA) [143, 144]	1971.80	0.22	6.152	6.209
RMF (NLZ2) [143, 144]	1969.22	0.274	6.251	6.333
MMM [51]	1968.5	0.22		
RMF (TMA) [145, 146]	1971.93	0.222	6.142	6.199
HFB-24 [148]	1968.45	0.26		
RMF (NL3) [147]	1974	0.26		
WS4 [152]	1970.27	0.217		
FRDM (2012) [153]	1971.48	0.222		
RCHB (PC-PK1) [122] 1)	1952.65		6.132	6.180
RCHB (PC-PK1) + RFB [162] 2)	1969.20		6.132	

Meng_Lu_Zhou2020
Sci. China-Phys. Mech. Astron. 63, 212011

Patyk_Sobiczewski1991

Ren…2002

Wu_Xu 2004

Geng… 2005; Geng2006

Zhang… 2012

Xia… 2018

Shi… 2019

^{270}Hs: ground state from MDC-RMF calc.

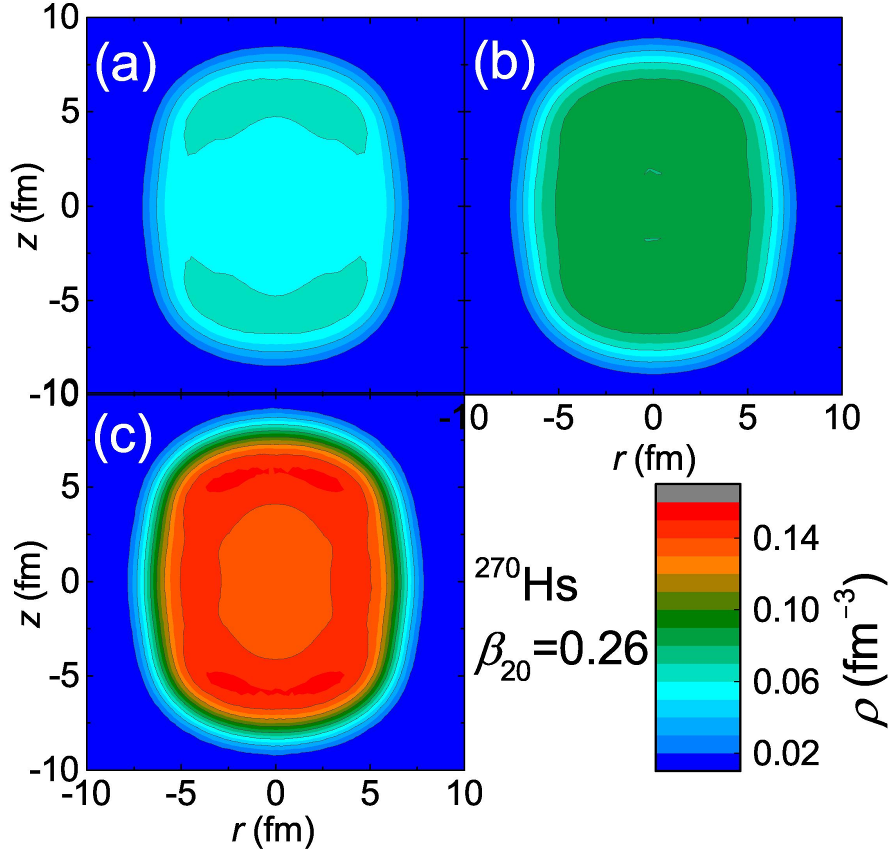

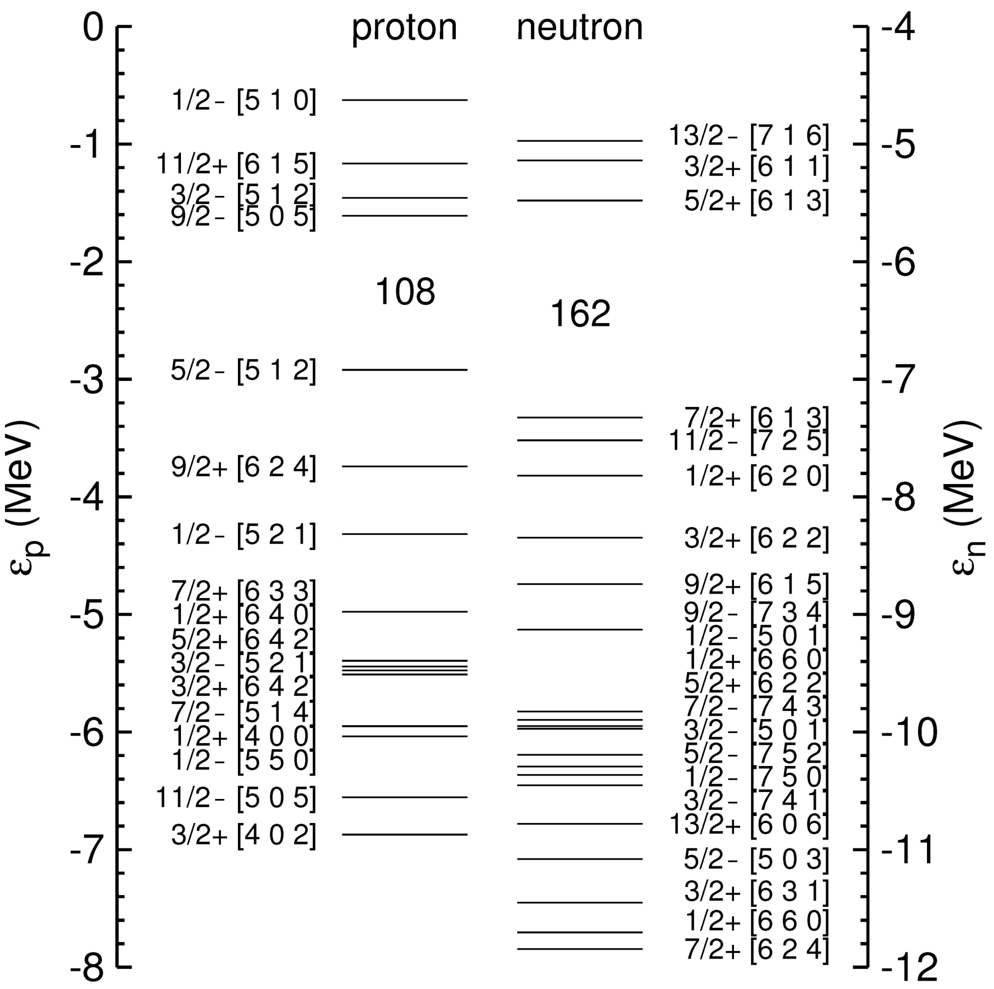

Xu Meng (孟旭), PhD thesis (2019)

Meng_Lu_Zhou2020
Sci. China-Phys. Mech. Astron. 63, 212011

Nuclear shapes

$$R(\theta,\varphi) = R_0 \left[1 + \beta_{00} + \sum_{\lambda=1}^{\infty} \sum_{\mu=-\lambda}^{\lambda} \beta^*_{\lambda\mu} Y_{\lambda\mu}(\theta,\varphi) \right]$$

2^λ-pole deformation (2^λ-极形变)

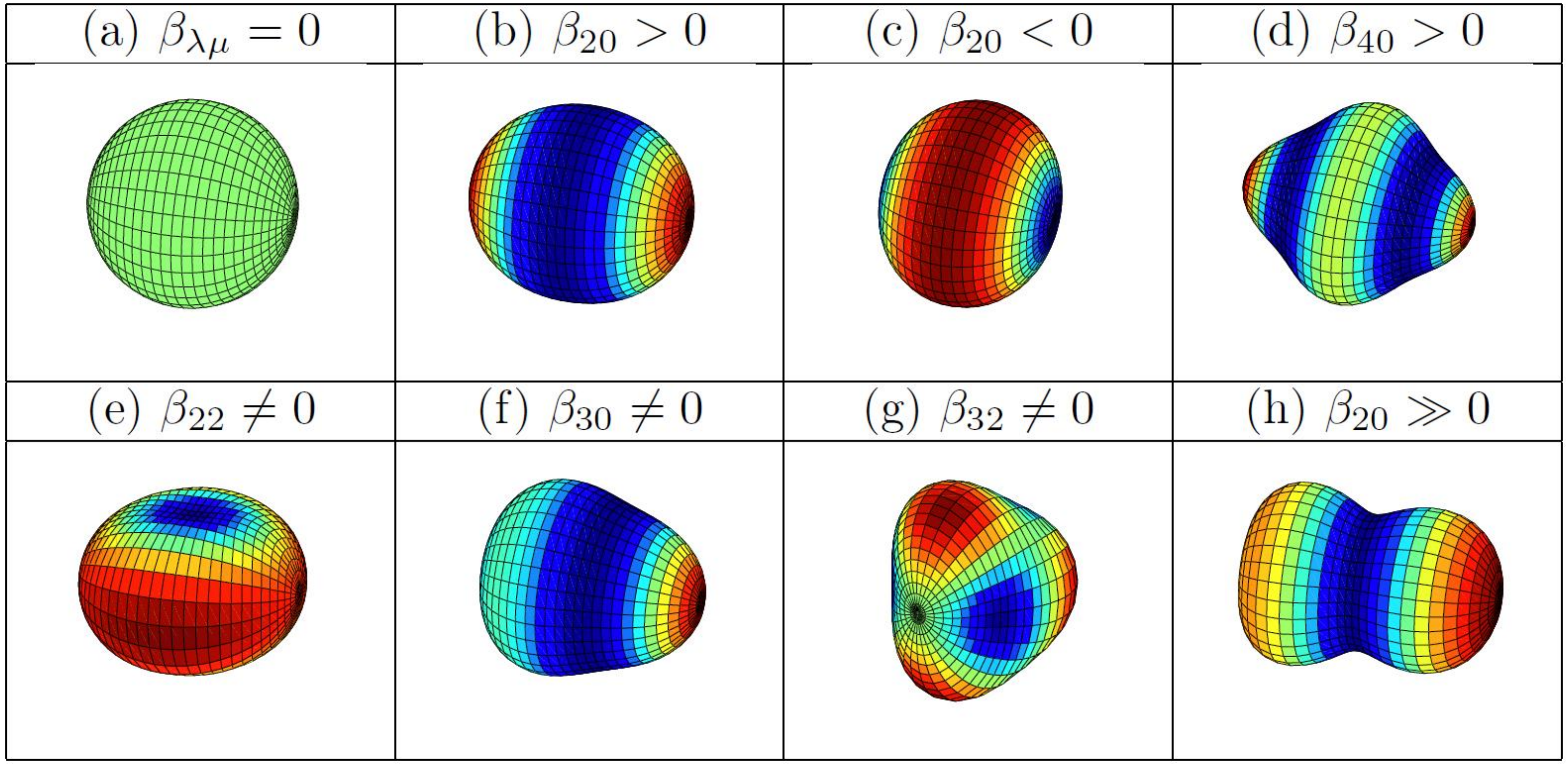

Courtesy of Bing-Nan Lu (吕炳楠)

Effects of higher-order deformations

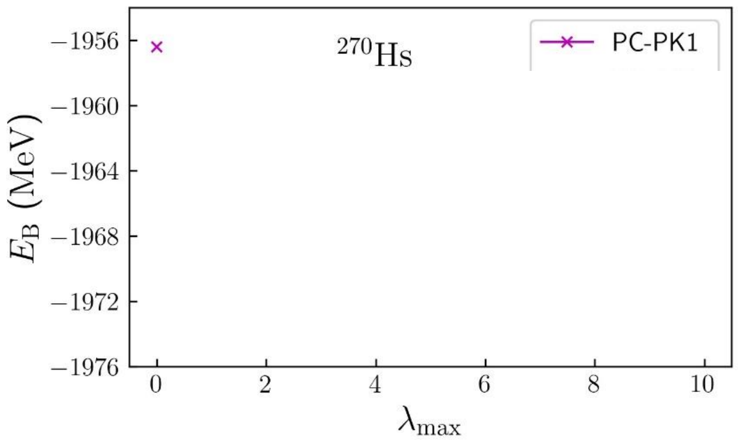

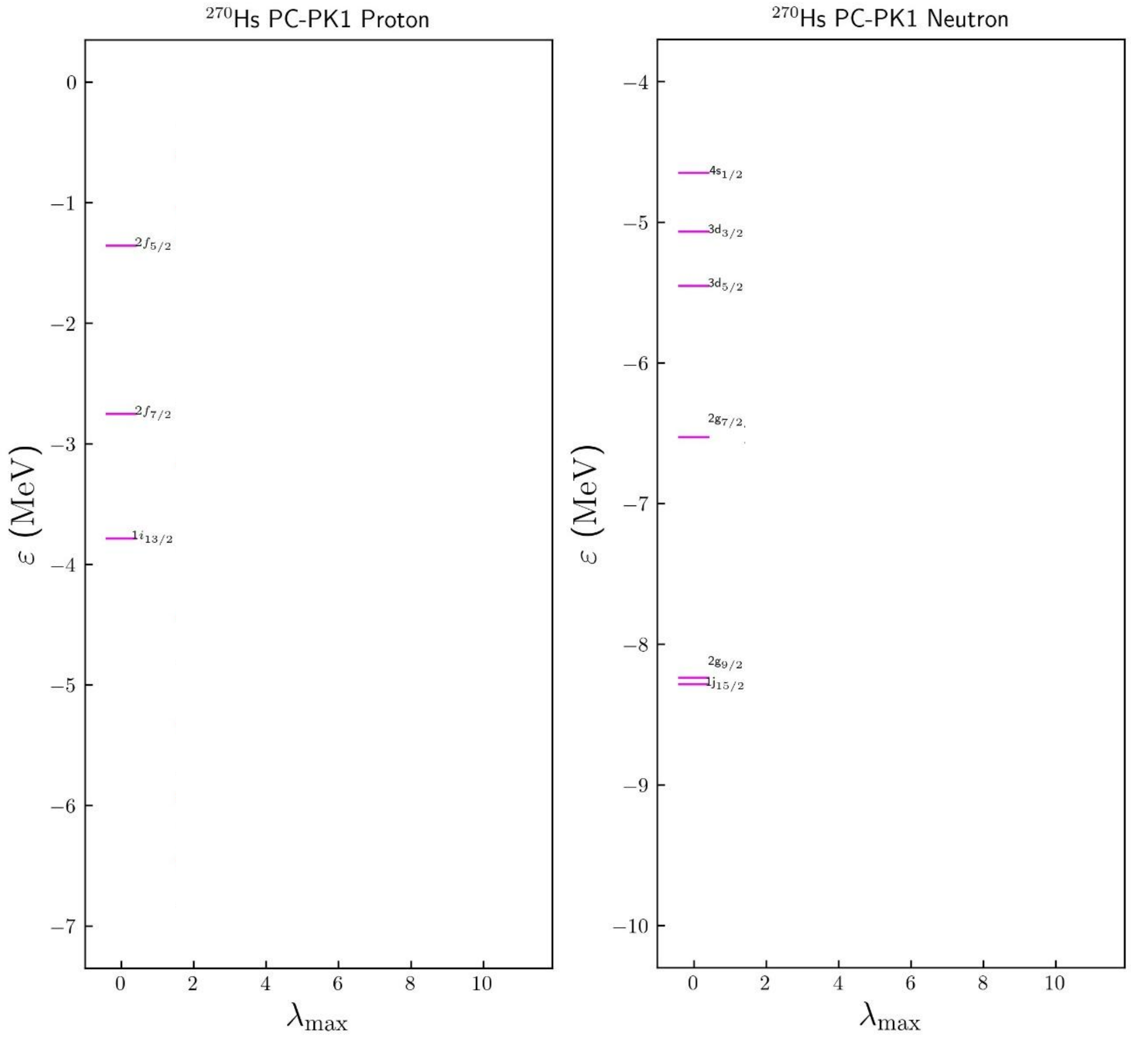

Courtesy of Xiao-Qian Wang (王晓倩)

$$R(\theta,\varphi) = R_0\left[1 + \beta_{00} + \sum_{\lambda=1}^{\infty}\sum_{\mu=-\lambda}^{\lambda}\beta^*_{\lambda\mu}Y_{\lambda\mu}(\theta,\varphi)\right]$$

Effects of higher-order deformations

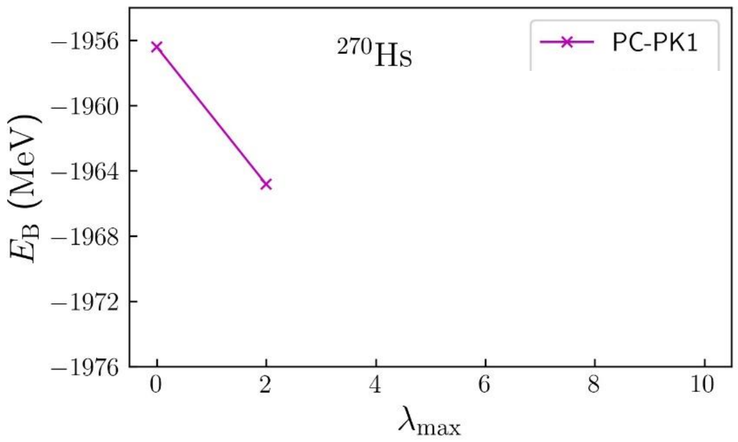

Changes in E_B & s.p. shell gap (in MeV)

λ_{max}	2	4	6	8	10
ΔE_B	8.43				
$\Delta^p{}_{sh}$	0.66				
$\Delta^n{}_{sh}$	1.17				

Courtesy of Xiao-Qian Wang (王晓倩)

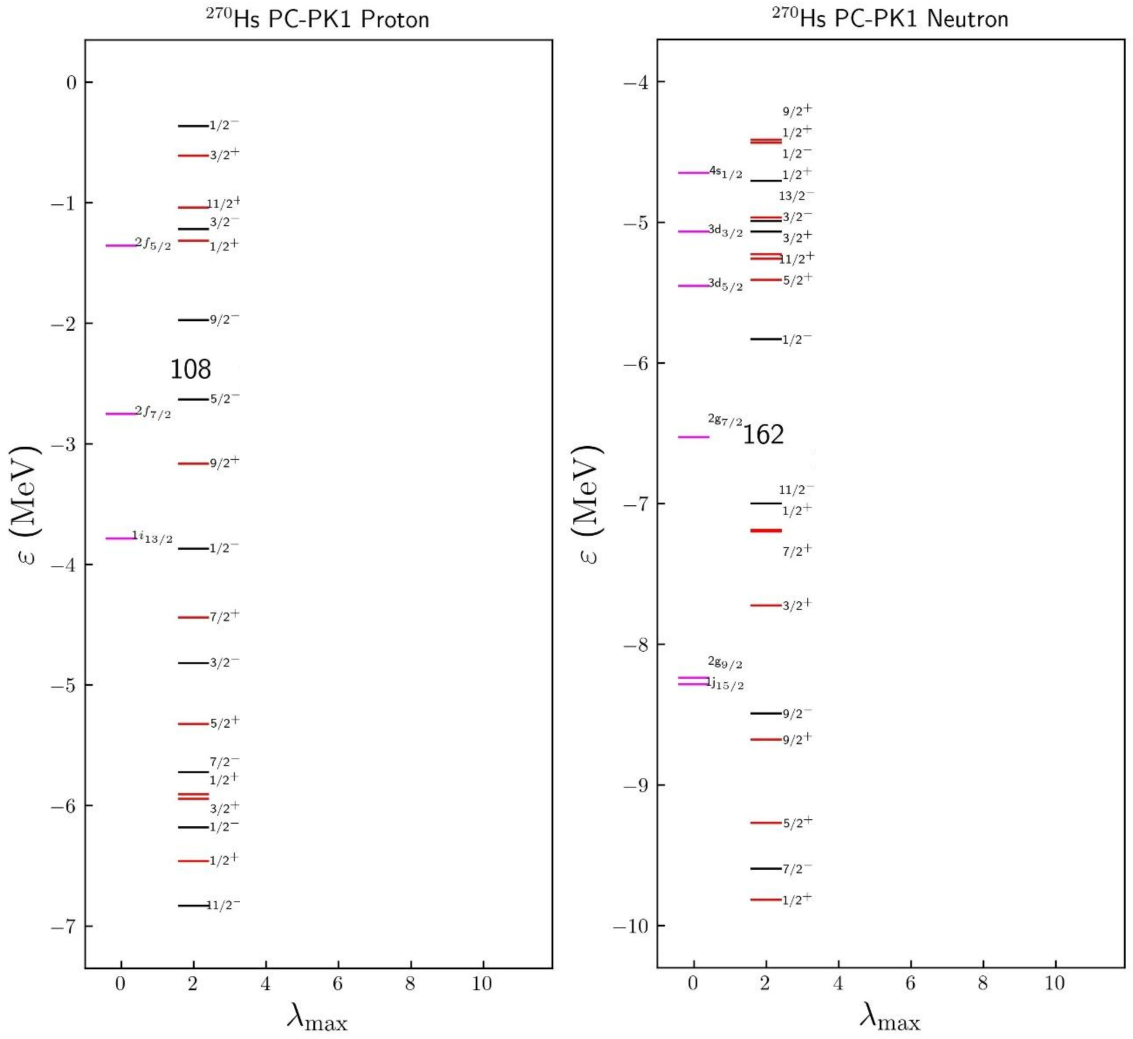

$$R(\theta,\varphi) = R_0\left[1 + \beta_{00} + \sum_{\lambda=1}^{\infty}\sum_{\mu=-\lambda}^{\lambda}\beta^*_{\lambda\mu}Y_{\lambda\mu}(\theta,\varphi)\right]$$

Effects of higher-order deformations

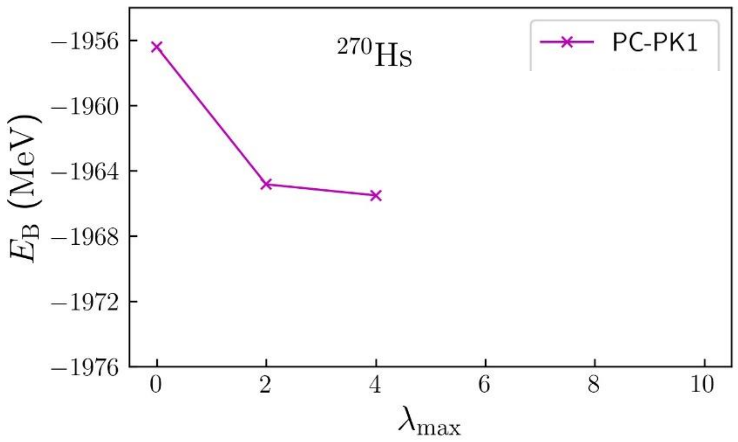

Changes in E_B & s.p. shell gap (in MeV)

λ_{max}	2	4	6	8	10
ΔE_B	8.43	0.68			
$\Delta^p{}_{sh}$	0.66	1.28			
$\Delta^n{}_{sh}$	1.17	1.56			

Courtesy of Xiao-Qian Wang (王晓倩)

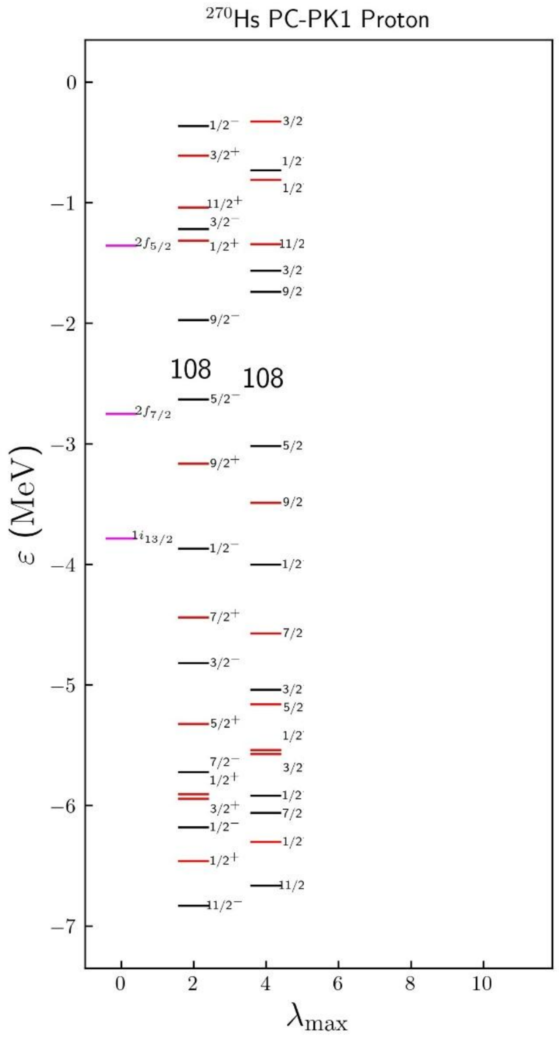

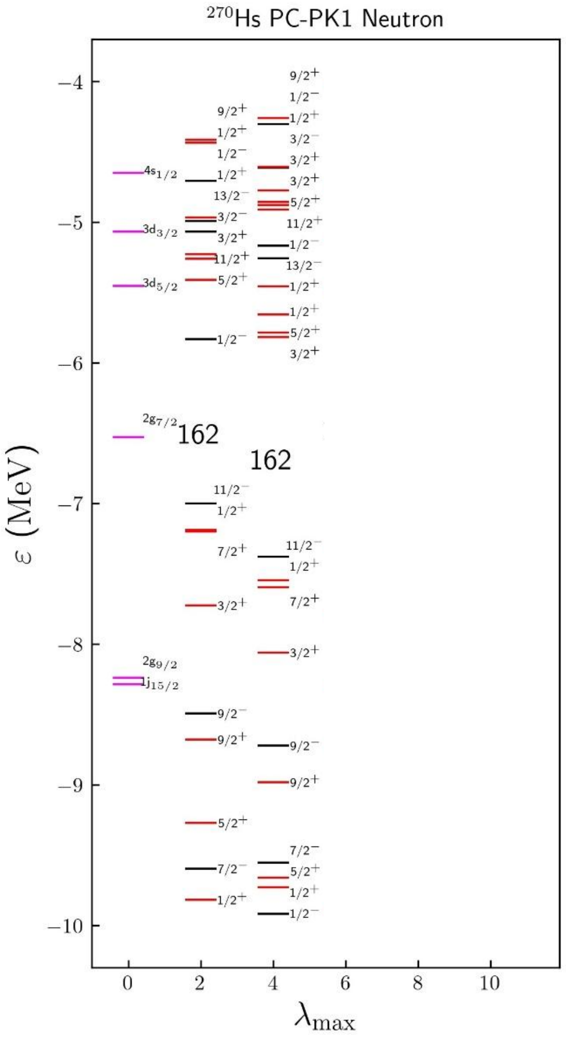

$$R(\theta,\varphi) = R_0\left[1 + \beta_{00} + \sum_{\lambda=1}^{\infty}\sum_{\mu=-\lambda}^{\lambda}\beta^*_{\lambda\mu}Y_{\lambda\mu}(\theta,\varphi)\right]$$

Effects of higher-order deformations

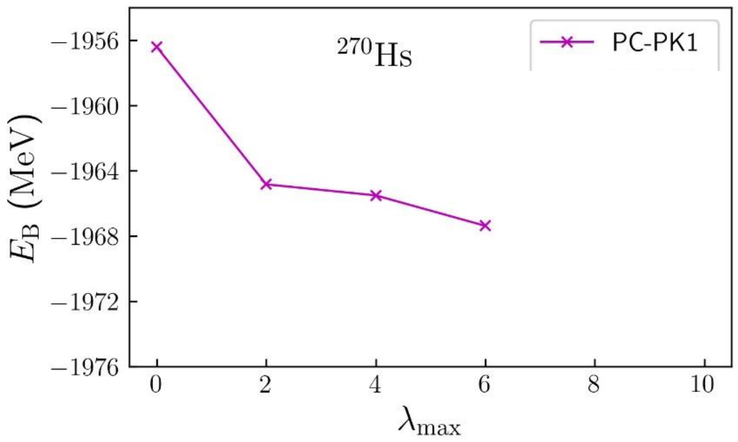

Changes in E_B & s.p. shell gap (in MeV)

λ_{max}	2	4	6	8	10
ΔE_B	8.43	0.68	1.87		
$\Delta^p{}_{sh}$	0.66	1.28	1.30		
$\Delta^n{}_{sh}$	1.17	1.56	1.84		

Courtesy of Xiao-Qian Wang (王晓倩)

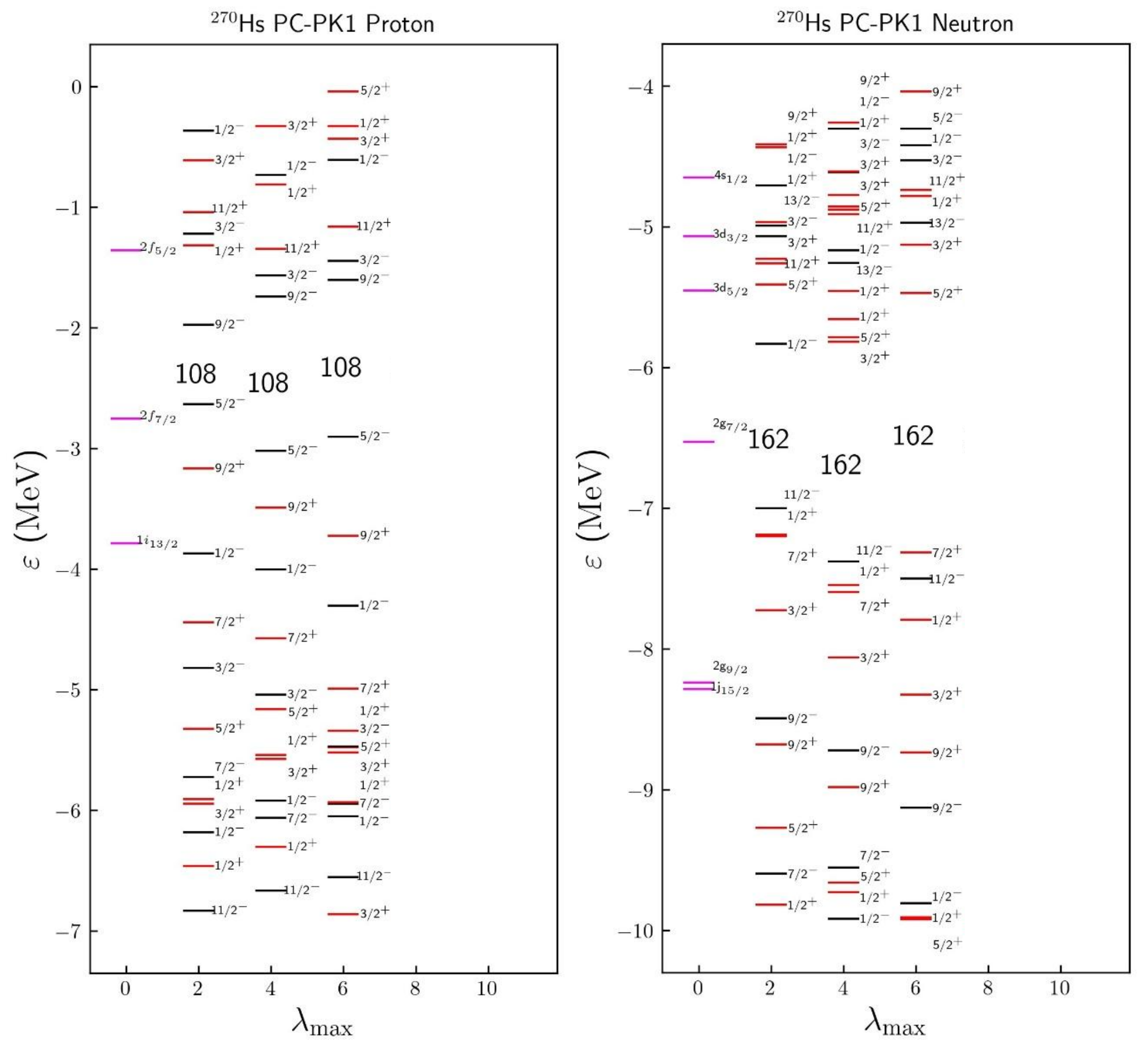

$$R(\theta,\varphi)=R_0\left[1+\beta_{00}+\sum_{\lambda=1}^{\infty}\sum_{\mu=-\lambda}^{\lambda}\beta^*_{\lambda\mu}Y_{\lambda\mu}(\theta,\varphi)\right]$$

Effects of higher-order deformations

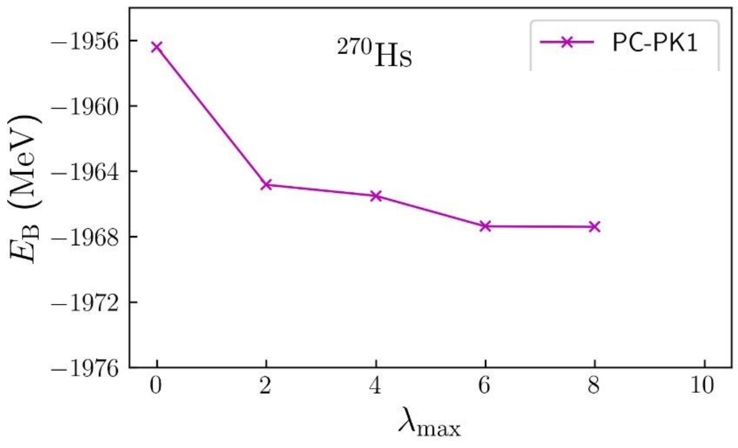

Changes in E_B & s.p. shell gap (in MeV)

λ_{max}	2	4	6	8	10
ΔE_B	8.43	0.68	1.87	0.03	
Δ^p_{sh}	0.66	1.28	1.30	1.34	
Δ^n_{sh}	1.17	1.56	1.84	1.85	

Courtesy of Xiao-Qian Wang (王晓倩)

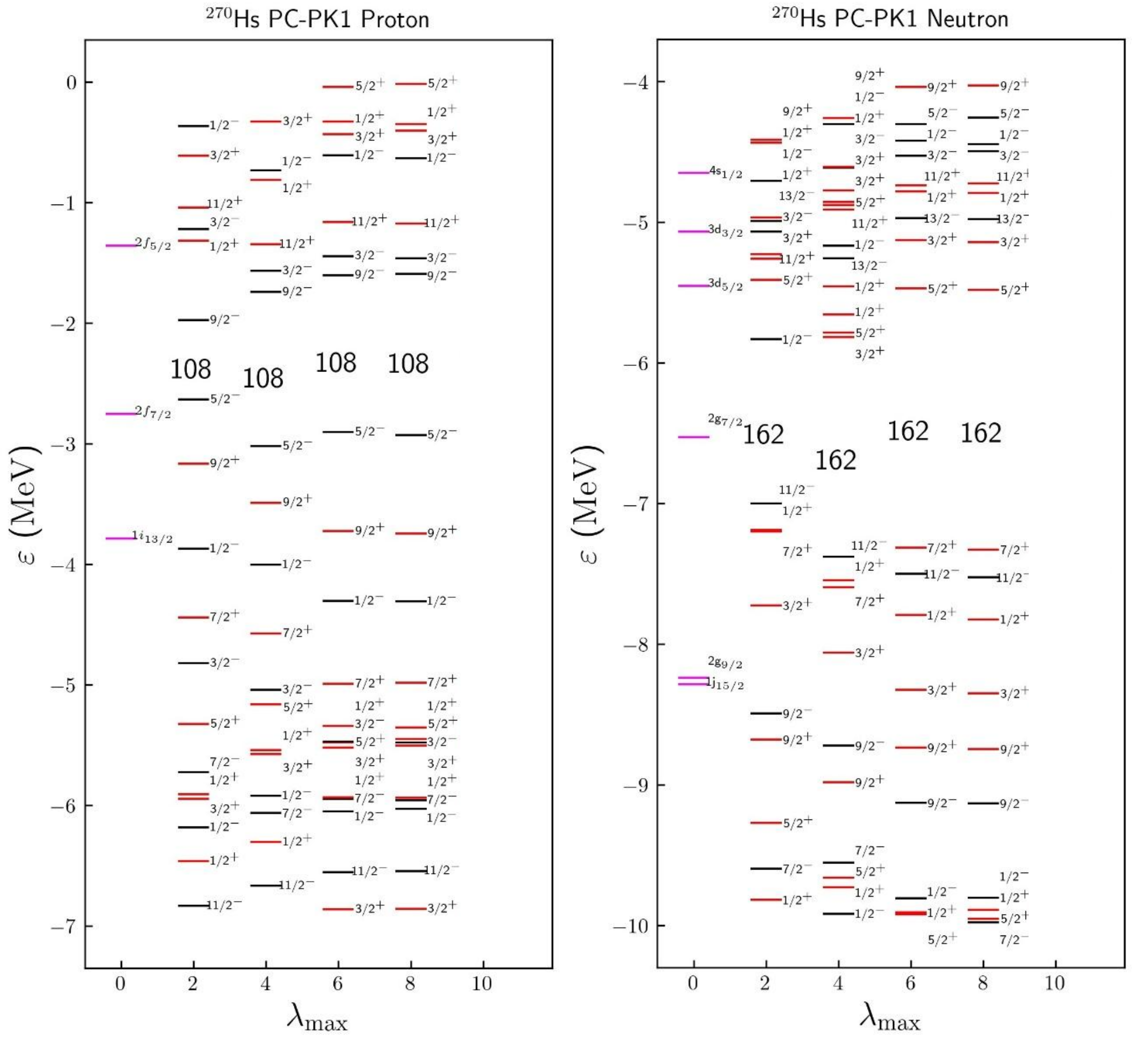

$$R(\theta,\varphi) = R_0\left[1+\beta_{00}+\sum_{\lambda=1}^{\infty}\sum_{\mu=-\lambda}^{\lambda}\beta^*_{\lambda\mu}Y_{\lambda\mu}(\theta,\varphi)\right]$$

Effects of higher-order deformations

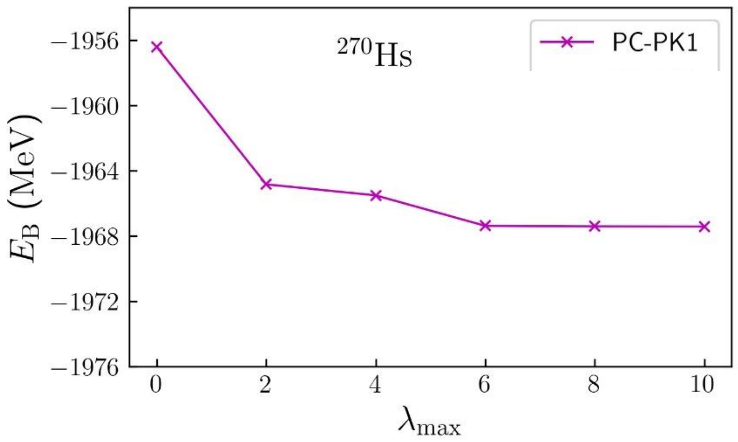

Changes in E_B & s.p. shell gap (in MeV)

λ_{max}	2	4	6	8	10
ΔE_B	8.43	0.68	1.87	0.03	0.01
Δ^{p}_{sh}	0.66	1.28	1.30	1.34	1.34
Δ^{n}_{sh}	1.17	1.56	1.84	1.85	1.85

Courtesy of Xiao-Qian Wang (王晓倩)

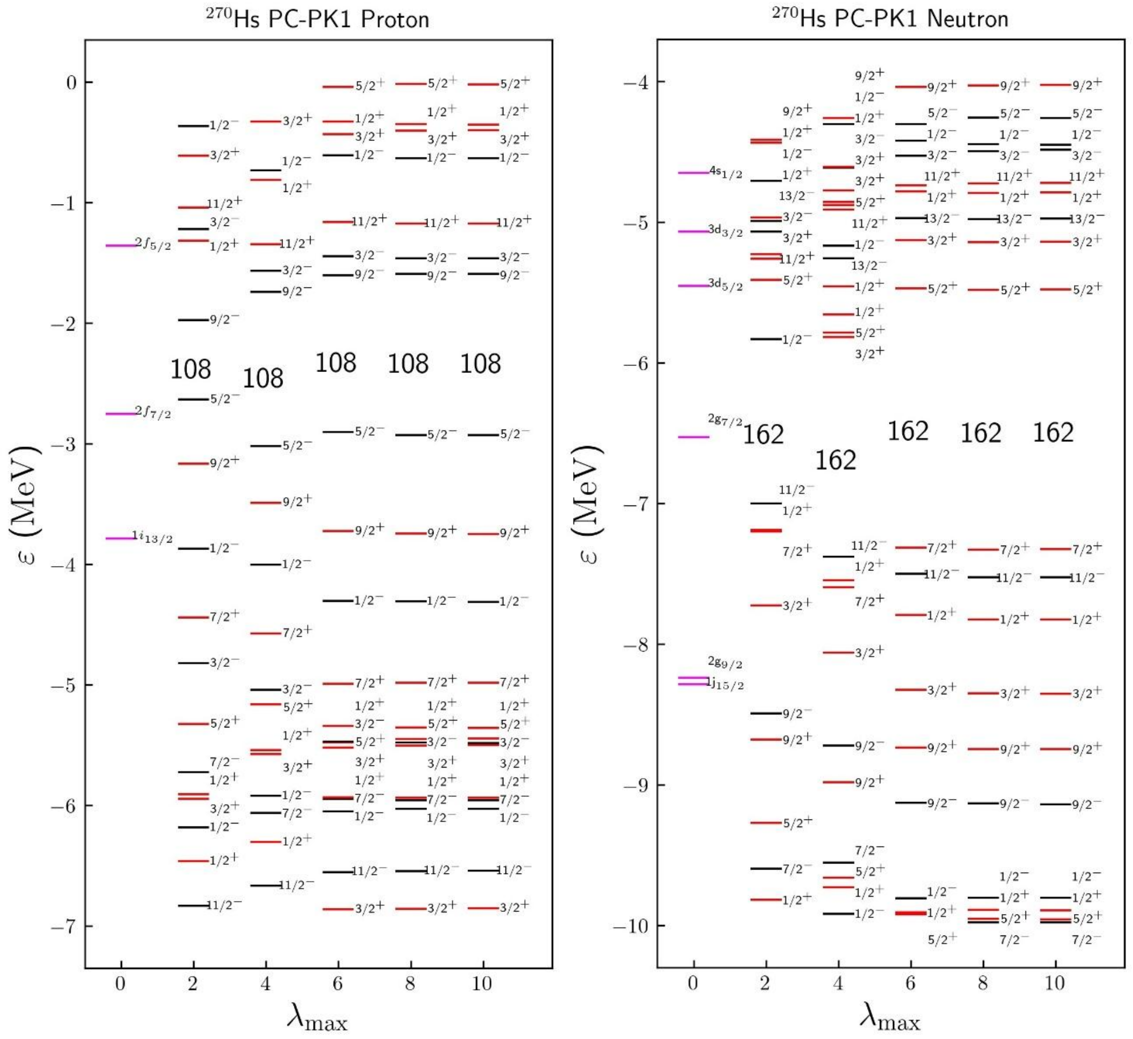

$$R(\theta,\varphi) = R_0\left[1 + \beta_{00} + \sum_{\lambda=1}^{\infty}\sum_{\mu=-\lambda}^{\lambda}\beta^{*}_{\lambda\mu}Y_{\lambda\mu}(\theta,\varphi)\right]$$

Effects of higher-order deformations

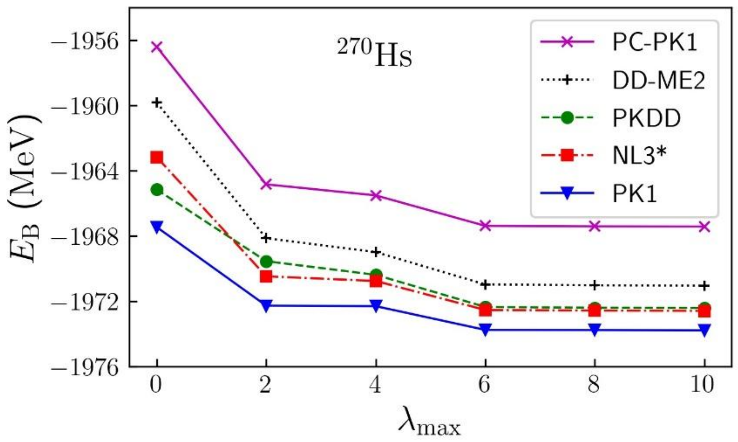

Changes in E_B & s.p. shell gap (in MeV)

λ_{max}	2	4	6	8	10
ΔE_B	8.43	0.68	1.87	0.03	0.01
Δ^p_{sh}	0.66	1.28	1.30	1.34	1.34
Δ^n_{sh}	1.17	1.56	1.84	1.85	1.85

Wang_Sun_SGZ2022_ChinPhysC46-024107

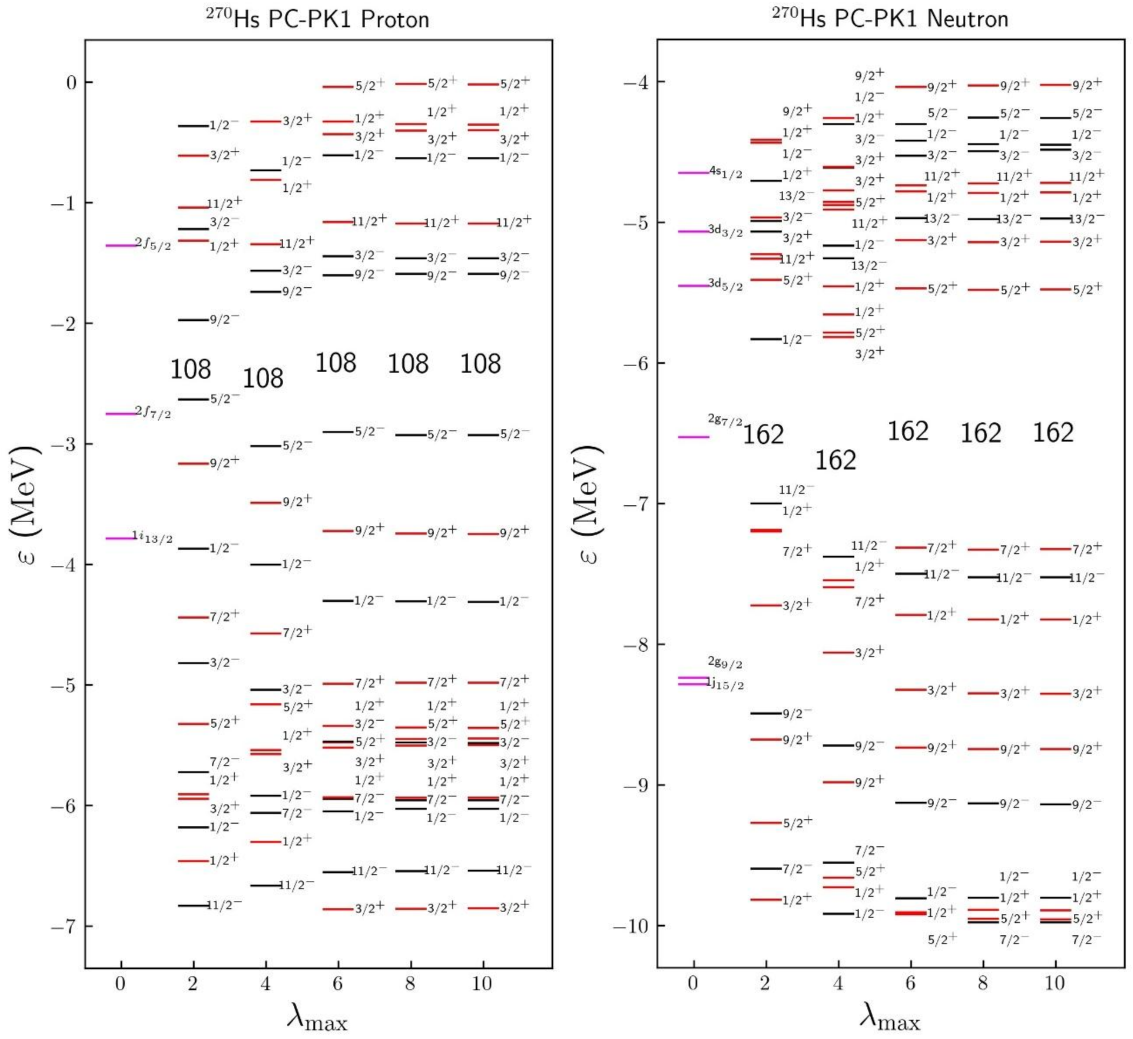

$$R(\theta,\varphi) = R_0\left[1 + \beta_{00} + \sum_{\lambda=1}^{\infty}\sum_{\mu=-\lambda}^{\lambda}\beta^*_{\lambda\mu}Y_{\lambda\mu}(\theta,\varphi)\right]$$

^{270}Hs: 1D PEC from MDC-RMF calc.

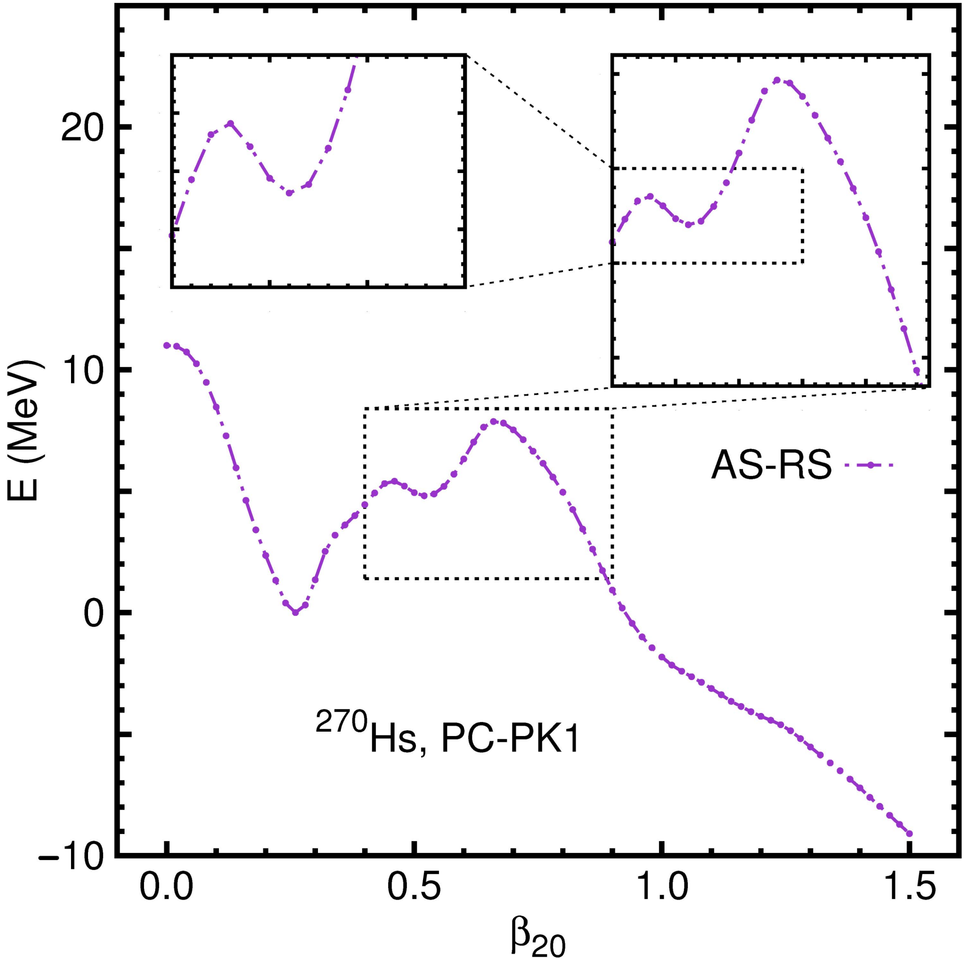

AS-RS: Axially-Symmetric & Reflection Symmetric

Courtesy of Xu Meng (孟旭)

^{270}Hs: 1D PEC from MDC-RMF calc.

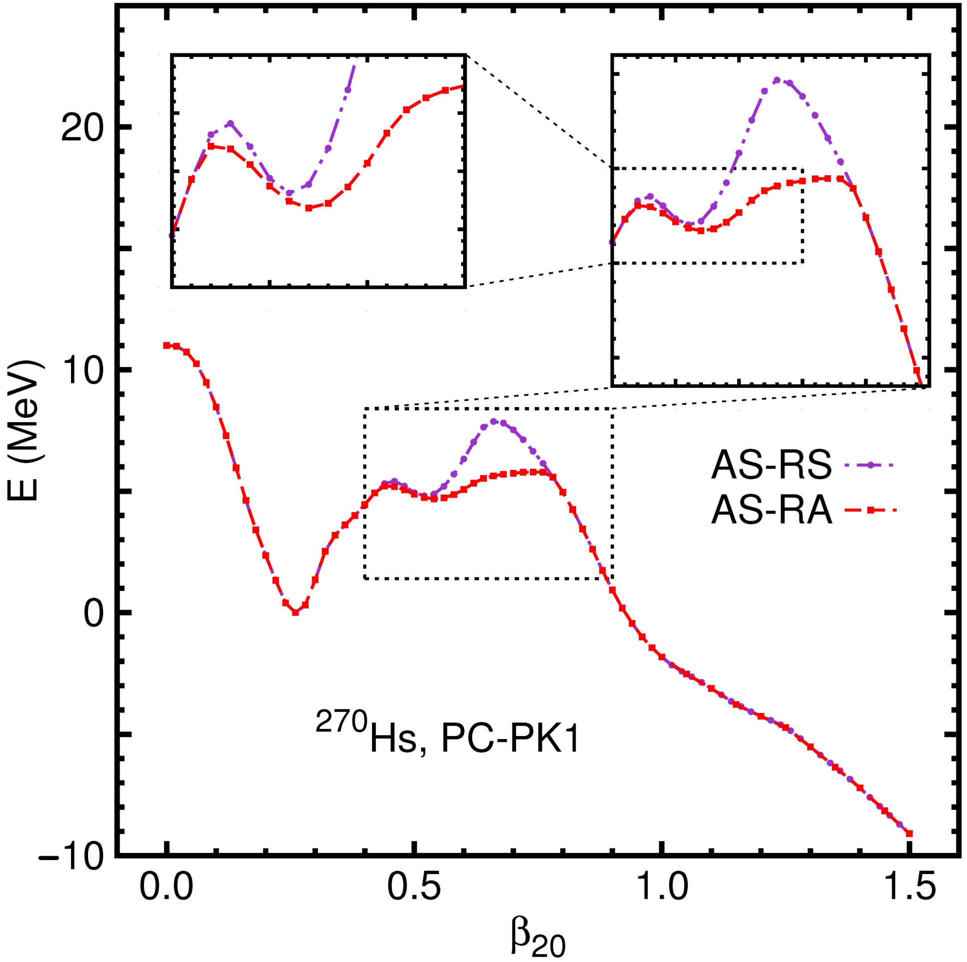

Courtesy of Xu Meng (孟旭)

AS-RS: Axially-Symmetric & Reflection Symmetric

AS-RA: Axially-Symmetric & Reflection Asymmetric

^{270}Hs: 1D PEC from MDC-RMF calc.

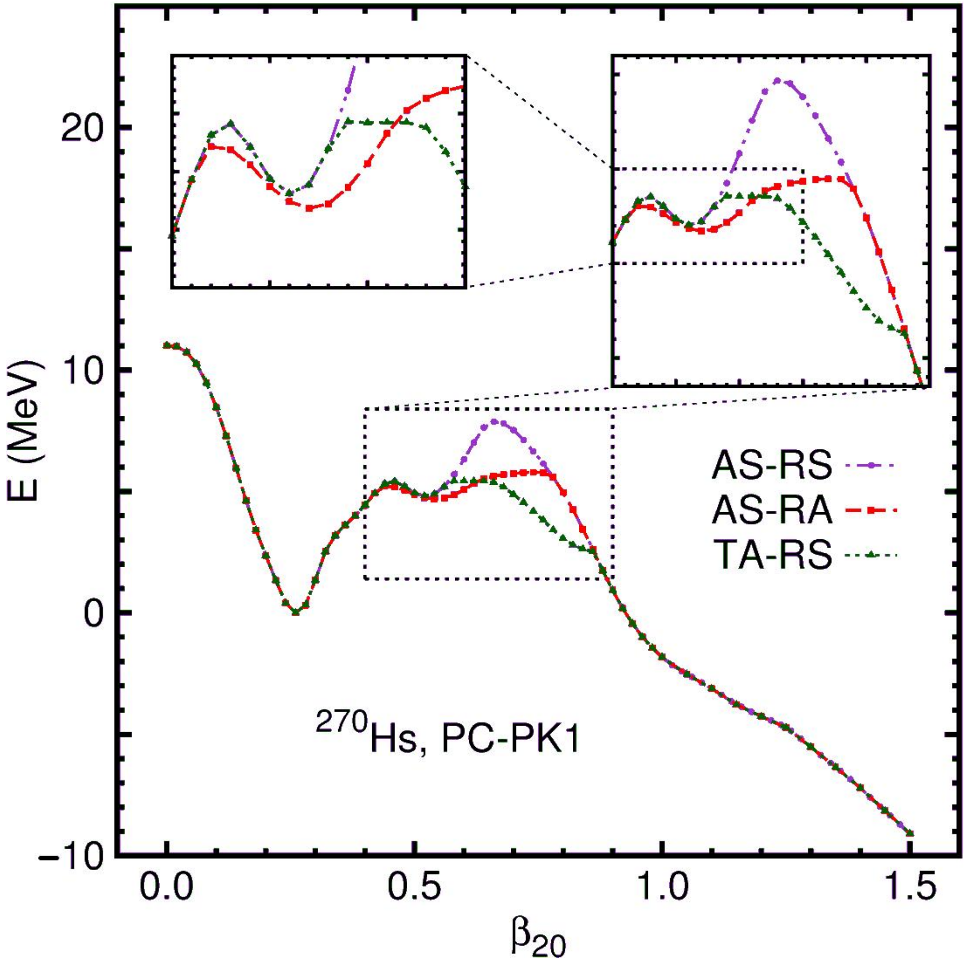

Courtesy of Xu Meng (孟旭)

AS-RS: Axially-Symmetric & Reflection Symmetric

AS-RA: Axially-Symmetric & Reflection Asymmetric

TA-RS: TriAxial & Reflection Symmetric

^{270}Hs: 1D PEC from MDC-RMF calc.

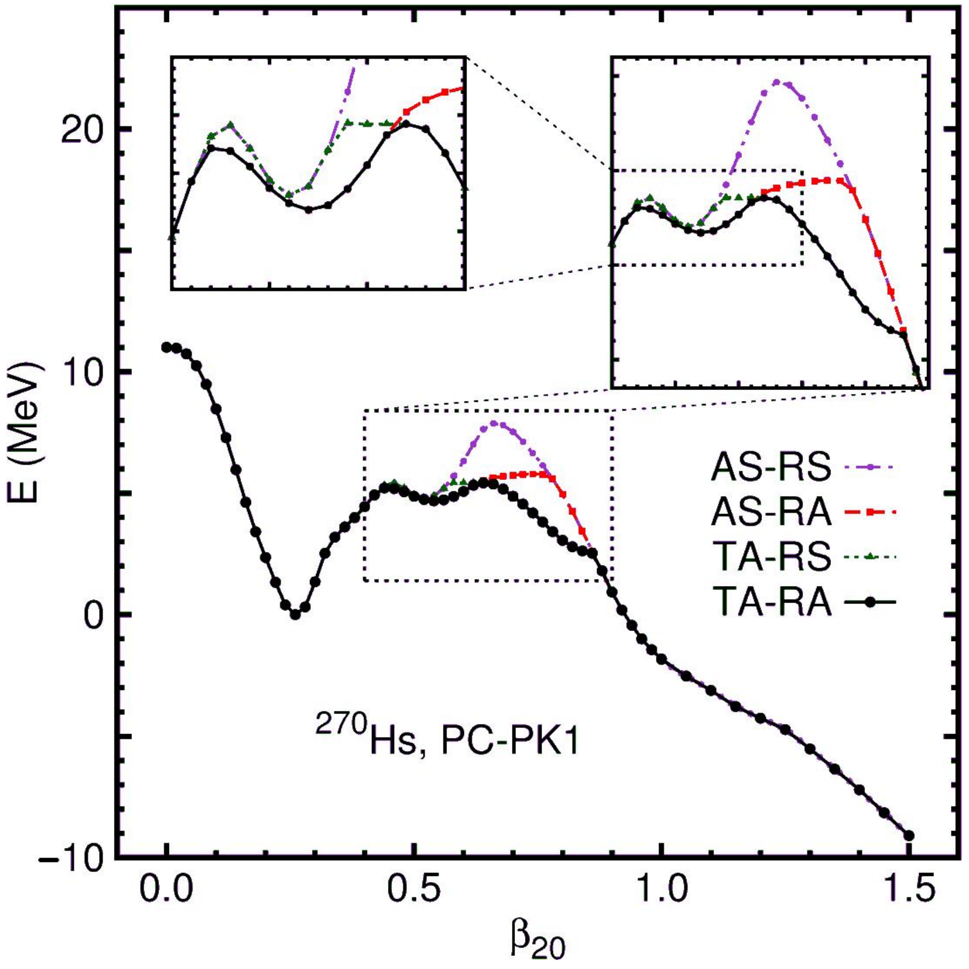

AS-RS: Axially-Symmetric & Reflection Symmetric

AS-RA: Axially-Symmetric & Reflection Asymmetric

TA-RS: TriAxial & Reflection Symmetric

TA-RA: TriAxial & Reflection Asymmetric

Meng_Lu_Zhou2020
Sci. China-Phys. Mech. Astron. 63, 212011

A systematic study of even-even superheavy nuclei

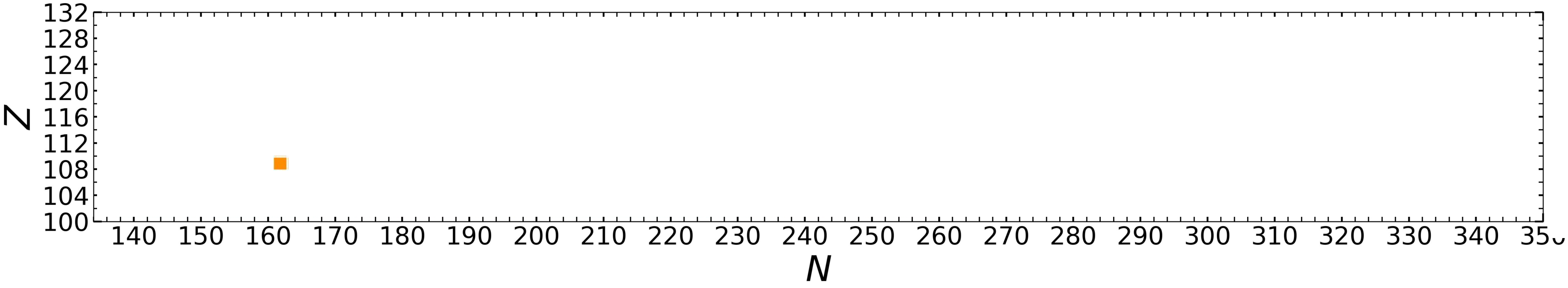

A systematic study of even-even superheavy nuclei

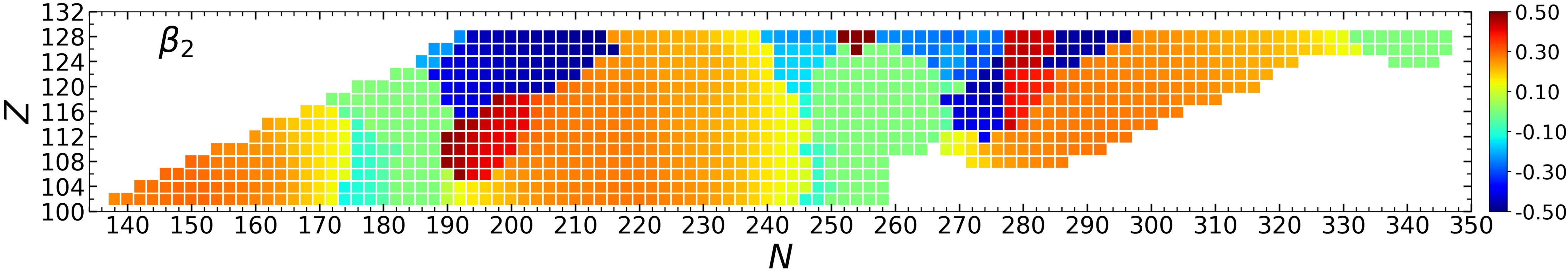

MDC-RMF calculations

- ➢ $102 \leq Z \leq 128$, proton drip line to neutron drip line
- ➢ Effective interaction: PC-PK1
- ➢ BCS w/ separable pairing force of finite range

Xiao-Qian Wang (王晓倩), PhD thesis (2024)

PECs of even-*N* Cn isotopes (160 ≤ *N* ≤ 288)

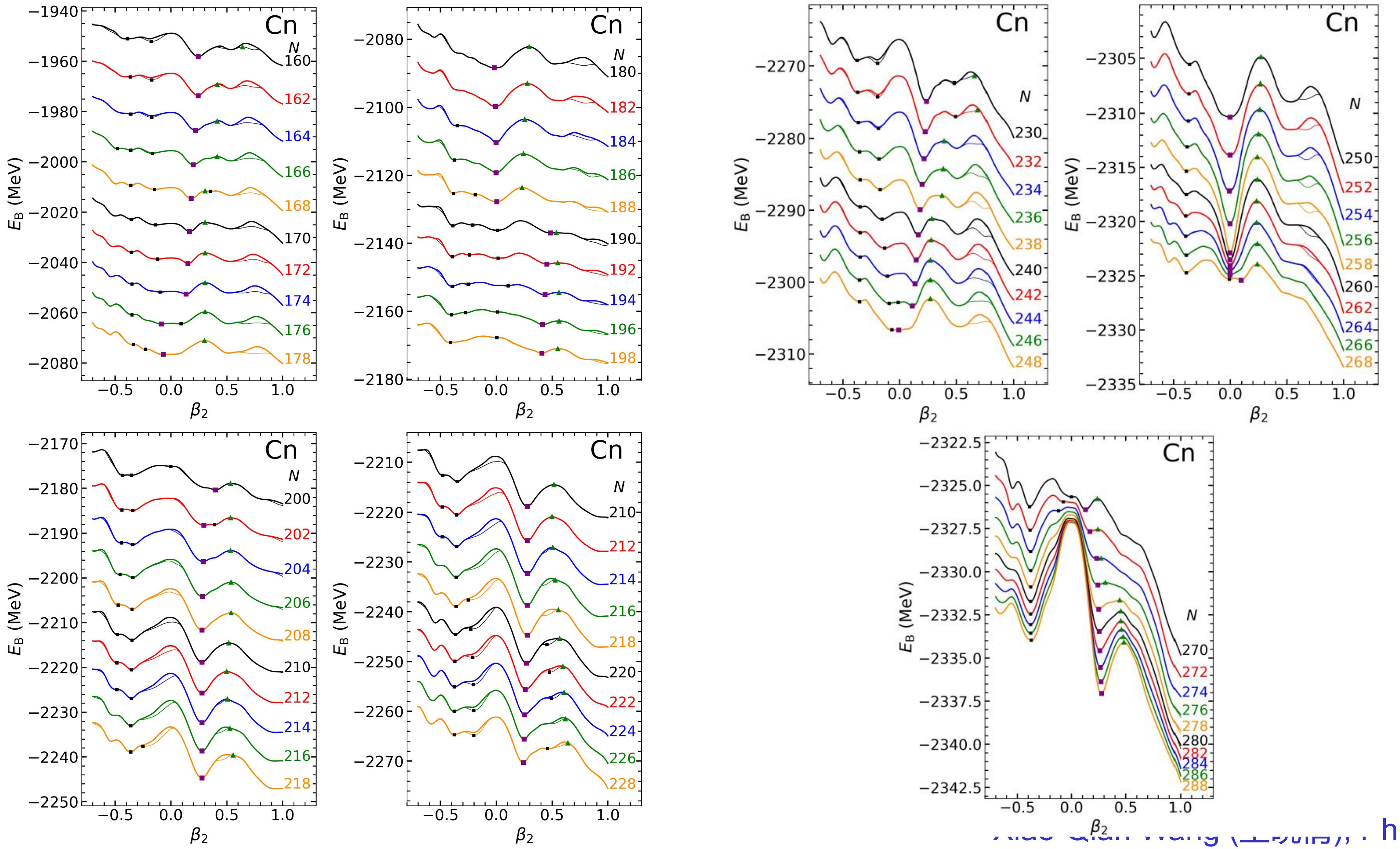

Xiao-Qian Wang, PhD thesis (2024)

PECs of ^{274}Cn

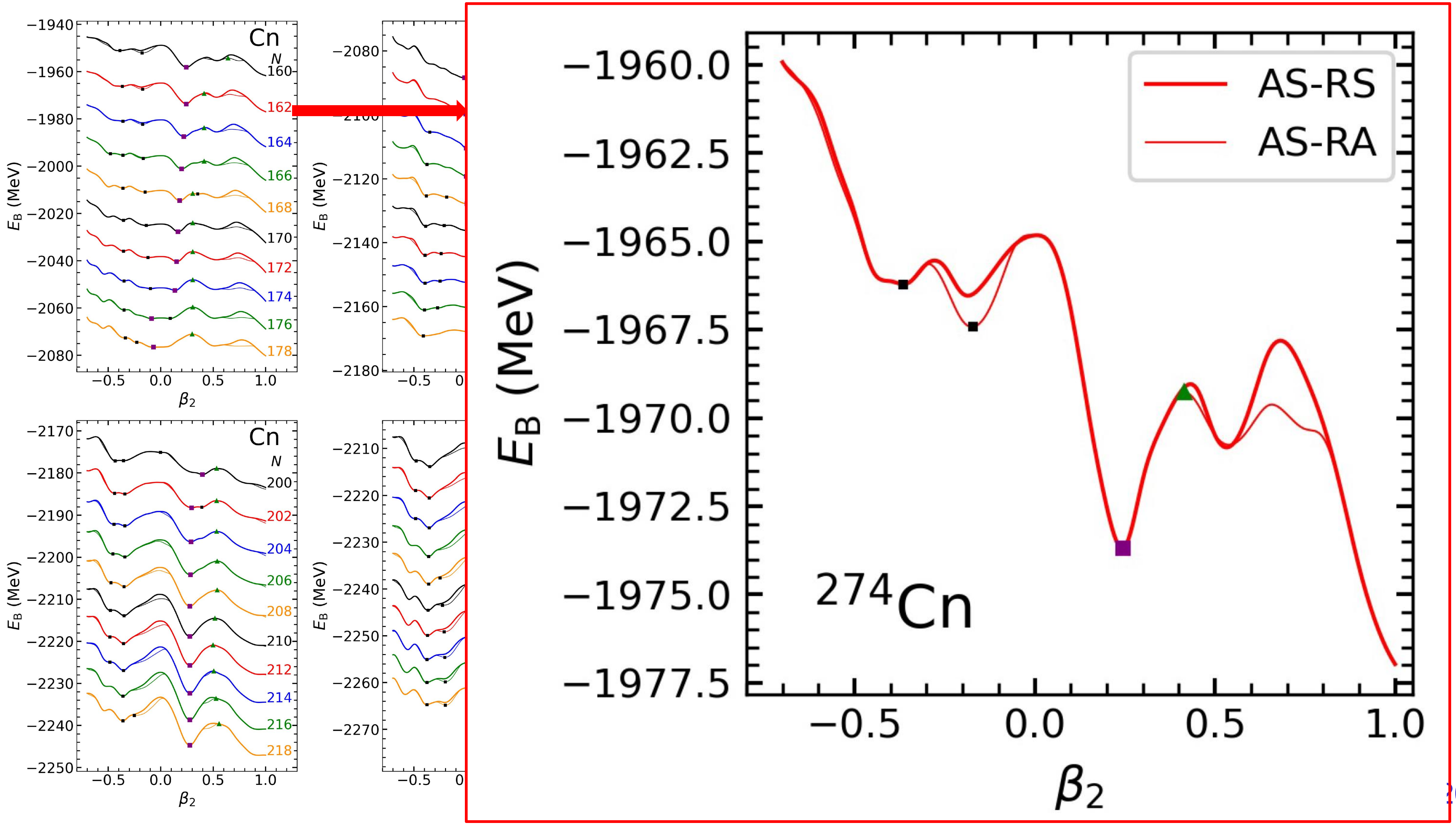

2024)

PECs of ^{282,284,286,288,290}Cn isotopes

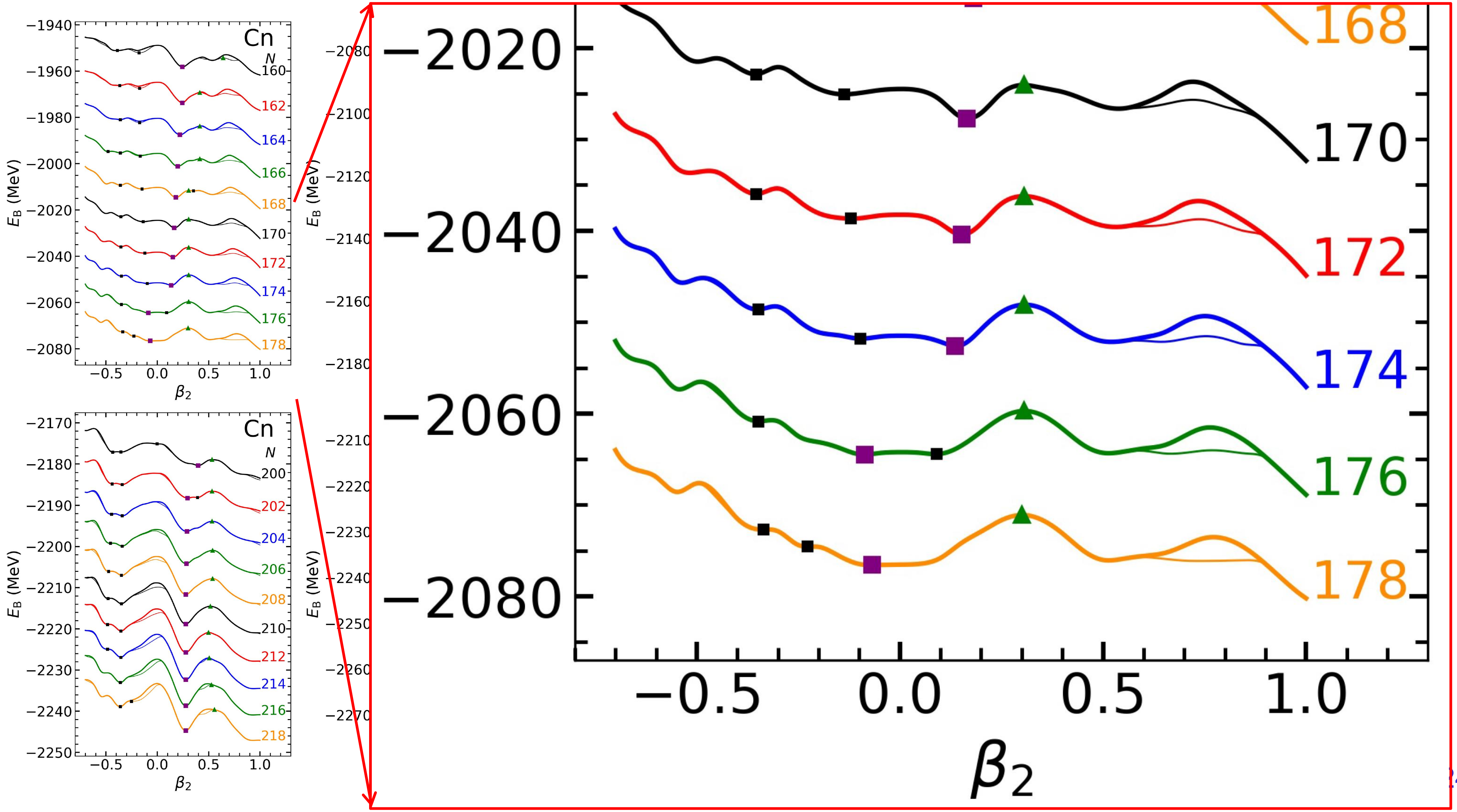

4)

A systematic study of even-even superheavy nuclei

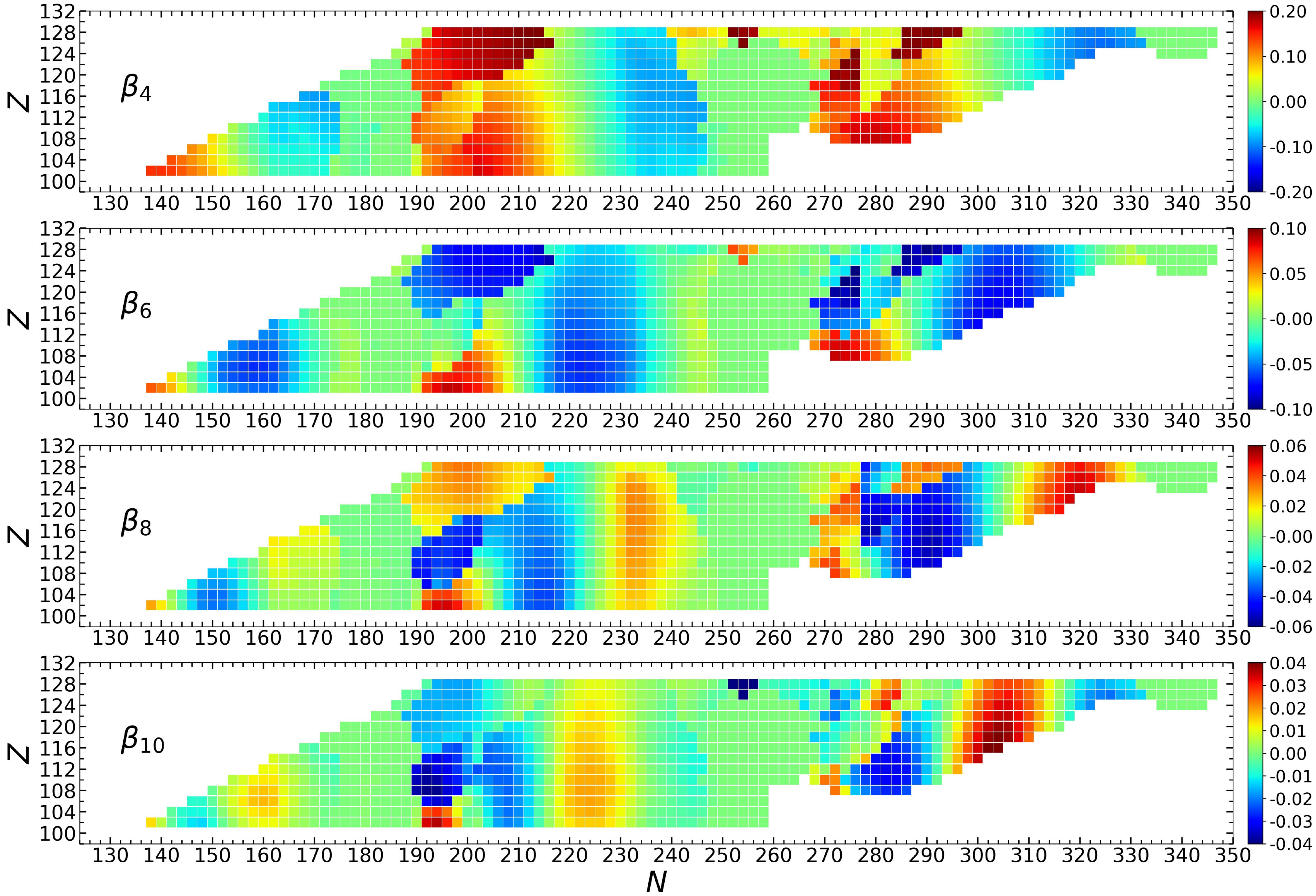

ıD thesis (2024)

Summary & perspectives

- Fission barrier is crucial for the description of fission & various shapes may appear during fission
- MultiDimensionally-Constrained Covariant Density Functional Theories
- Potential energy surfaces & fission barriers: ^{240}Pu; actinides & ^{270}Hs; superheavies
  - Inner barrier: triaxial deformation
  - Outer barrier: octupole & triaxial deformations
  - A systematic study of even-even superheavy nuclei (w/o triaxiality)

Summary & perspectives

- Fission barrier is crucial for the description of fission & various shapes may appear during fission
- MultiDimensionally-Constrained Covariant Density Functional Theories
- Potential energy surfaces & fission barriers: ^{240}Pu; actinides & ^{270}Hs; superheavies
  - Inner barrier: triaxial deformation
  - Outer barrier: octupole & triaxial deformations
  - A systematic study of even-even superheavy nuclei (w/o triaxiality)

Thank you !